DEVELOPMENT OF AN EFFICIENT ANCHORAGE MECHANISM FOR RC BEAM-COLUMN JOINTS

Thesis Submitted to AcSIR for the Award of

the Degree of

MASTER OF TECHNOLOGY

in

BUILDING ENGINEERING AND DISASTER MITIGATION

by

ASHISH KUMAR GUPTA

30EE15A01001

Under the Guidance of

Dr. Ajay Chourasia

Dr. S. K. Panigrahi

CSIR-Central Building Research Institute

Roorkee-247667

May, 2017

CERTIFICATE

This is to certify that the work incorporated in this M. Tech. thesis entitled "*Development of an Efficient Anchorage Mechanism for RC Beam-Column Joints*" submitted by *Mr. Ashish Kumar Gupta* to Academy of Scientific and Innovative Research (AcSIR) in fulfilment of the requirements for the award of the Degree of *Master of Technology*, embodies original research work under our guidance. We further certify that this work has not been submitted to any other university or institution in part or full for the award of any degree or diploma. Research material obtained from other sources has been duly acknowledged in the thesis. Any text, illustration, table etc., used in the thesis from other sources, have been duly cited and acknowledged.

Ashish Kumar Gupta 15/05/17

(Ashish Kumar Gupta)
M. Tech. Student
AcSIR
CSIR-CBRI
Roorkee-247667, India

(Dr. Ajay Chourasia)
Associate Professor
AcSIR
CSIR-CBRI
Roorkee-247667, India

Shpanigrahi 15/5/17

(Dr. S. K. Panigrahi)
Associate Professor
AcSIR
CSIR-CBRI
Roorkee-247667, India

ACKNOWLEDGEMENT

I thank almighty God for helping me one way or the other and providing strength to me all the time.

It is my great pleasure to express my indebtedness to my supervisors, Dr. Ajay Chourasia, Principal Scientist, SE Group, CSIR-CBRI, Roorkee and Dr. S. K. Panigrahi, Principal Scientist, AIMS Group, CSIR-CBRI, Roorkee, whose encouragement and continuous support has made it possible to complete this work in its present form.

It is my great pleasure to acknowledge the Director, CSIR-CBRI, Roorkee for his generous support to accomplish my project work.

I wish to acknowledge, Dr. S. R. Karade, Senior Principal Scientist, OBM Group, CSIR-CBRI, Roorkee, Mrs. Shermi C., Scientist, SE Group, CSIR-CBRI, Roorkee, Mr. Chanchal Sonkar, Scientist, SE Group, CSIR-CBRI, Roorkee, Mr. Srinivasa Rao Naik B., Scientist, EST Group, CSIR-CBRI, Roorkee, Mr. Manojit Samanta, Scientist, GE Group, CSIR-CBRI, Roorkee, Mr. Bibekananda Mandal, PhD Scholar, IIT Roorkee, Mr. Jalaj Parashar, Senior Technical Officer, SE Group, CSIR-CBRI, Roorkee, Mr. Monu Kumar, Project Assistant, CSIR-CBRI, Roorkee, Ms. Neelam Chauhan, Project Assistant, CSIR-CBRI, Mr. Jaipal Saini, Sr. Technician, OBM Group, CSIR-CBRI, Roorkee for their support, encouragement and guidance that helped me during my project work. I am grateful to my seniors Mr. Mahesh Sharma, Mr. Shiv Singh Patel, Mr. Ravi Kumar, Mr. Rohit Kumar, Mr. Piyush Punetha, Mr. Arpit Goyal and my batch mates Mr. Anujay Rawat and Mr. A.V.S. Ramakrishna for their support and fruitful advice.

I am greatly thankful to my family members whose constant support give me the strength to complete my work.

Date: 15-05-2017

Place: Roorkee

Ashish Kumar Gupta

ASHISH KUMAR GUPTA

ABSTRACT

The present method of anchorage (90^o or 180^o bent bar) used at beam-column joint creates congestion causing improper bending of large diameter bar and honeycombing of concrete. The use of mechanical anchor at the end of the bar (headed bar) could be an attractive alternative to the conventional method, to reduce the congestion at the beam-column joints. Hence, there is a need to develop an effective headed bar which is easy to use. The present study was thus focused on the development of a headed bar which will fulfil the aforesaid requirements. To achieve the present objective, numerical analysis and experimental investigations were carried out to determine the maximum pull-out capacity of the headed bar with different mechanical anchors. A total of fifteen different mechanical anchors were used having lengths of 11 mm, 19 mm, 27 mm, 35 mm and 43 mm having deformations over the length of anchor such as plain, grooved and ribbed.

In the first phase of study, numerical analysis of the pull-out behaviour with headed bar were done using ABAQUS software based on finite element analysis. There were 15 different types of analysis were done with the different types of mechanical anchor. The variables are considered as length of mechanical anchor and deformation over the length of mechanical anchor. The embedment depth, diameter of anchor, diameter of reinforcement, grade of steel reinforcement, grade of steel used for mechanical anchor, grade of concrete, size of concrete cube were taken constant during the analysis. The results showed that the variation in the length of the mechanical has very less effect on the pull-out capacity. For plain bar and grooved head, the maximum pull-out capacity was found for 19 mm length of mechanical anchor while for ribbed head it was found for 11 mm. The deformation over the length of mechanical anchor has also very less effect on the pull-out capacity of the headed bar.

In the second phase of study, experimental investigation were carried out with the same specifications as mentioned in the numerical analysis. Over fifty concrete cube specimen with headed bar were cast for pull-out testing in order to determine the effect of several variables. These variables include, length of anchor and deformation over the length of anchor. It was found that failure was bar fracture when headed bar were used while slippage of bar occurred in absence of anchor. From the result, it has been observed that the headed bar can be used over straight bar having several advantages such as reduced congestion, lower bond slip and greater pull-out capacity. The results of the analysis provides the understanding of the different mechanical anchors which will be appropriate for the beam-column joint.

CONTENTS

CERTIFICATE..... i

ACKNOWLEDGEMENT.....ii

ABSTRACT..... iii

CONTENTS..... iv

LIST OF FIGURES..... viii

LIST OF TABLES..... xi

CHAPTER 1: INTRODUCTION.....**1-3**

1.1 Backdrop 1

1.2 Research significance 1

1.3 Research objective.....2

1.4 Research methodology 2

1.5 Organization of the thesis.....3

CHAPTER 2: LITERATURE REVIEW.....**4-31**

2.1 Bond and force transfer mechanism.....4

2.2 Development length formulation 6

2.2.1 Indian Standards.....6

2.2.2 ACI Standards 7

2.3 Beam column joint 7

2.3.1 General.....7

2.4 Design considerations for beam-column joint 11

2.4.1 General.....11

2.4.2 Conventional Methods 11

2.4.3 Mechanical anchors.....11

2.5 Headed bars 12

2.5.1 Background 12

2.5.2 Previous research 13

2.5.3 Factors affecting anchorage capacity of headed bars.....20

2.5.4 Summary of codal provisions 25

2.6 Patents registered 30
2.7 Indian Scenario 31
2.8 Concluding remarks 31
CHAPTER 3: MATERIAL CHARACTERISATION 32-39
3.1 General 32
3.2 Concrete and its constituents 32
3.2.1 Cement 32
3.2.2 Fine aggregates 33
3.2.3 Coarse aggregates 34
3.2.4 Water 37
3.2.5 Concrete mix proportion 37
3.3 Properties of headed bar 38
3.3.1 Reinforcement steel 38
3.3.2 Mechanical anchors 39
CHAPTER 4: NUMERICAL ANALYSIS 40-55
4.1 Introduction 40
4.2 Finite element analysis 41
4.2.1 Modeling strategies 41
4.2.2 Element types 43
4.2.3 Material properties 43
4.2.4 Concrete damage plasticity 46
4.2.5 Loading 47
4.2.6 Model convergence 48
4.2.7 Interaction 48
4.2.8 Meshing or discretization 48
4.2.9 Boundary conditions 49
4.2.10 Failure type 49
4.2.11 Validation of model 49
4.2.12 Modeling of test specimens 51
4.2.13 Notation of the anchor 54
4.3 Limitations 55

4.4 Summary 55

CHAPTER 5: EXPERIMENTAL INVESTIGATION 56-66

5.1 Introduction 56

5.2 Development of headed bar 56

5.2.1 Fabrication and assembling 56

5.2.2 Concrete cube specimen 58

5.3 Curing of specimen 61

5.4 Test setup 61

5.5 Instrumentation and measurement 64

5.5.1 Installation of strain gauges 64

5.5.2 Measurement of strain 65

5.5.3 Measurement of force and displacement 65

5.6 Test procedure 66

CHAPTER 6: RESULTS AND DISCUSSION 68-79

6.1 General 68

6.2 Numerical results 68

6.2.1 Effect of length of mechanical anchor on pull-out capacity 68

6.2.2 Effect of deformation over the length of mechanical anchor on pull-out capacity 70

6.2.3 Behaviour of initial cracking to ultimate failure 72

6.3 Experimental results 74

6.3.1 Pull-out test result with anchor 74

6.3.2 Pull-out result without anchor 77

6.3.3 Comparison of results of with and without anchor 78

6.3.4 Effect of length and deformation over length of anchor on pull-out capacity 78

6.4 Comparison of numerical and experimental results 79

CHAPTER 7: CONCLUSIONS AND FUTURE SCOPE OF WORK 80-81

7.1 Summary 80

7.2 Conclusions 80

7.3 Future scope of work 81

REFERENCES..... **83-87**

LIST OF FIGURES

Figure 2.1: Different forces generated after applying external force 4
Figure 2.2: Force transfer mechanism 5
Figure 2.3: Schematic view showing development length of bar in concrete 6
Figure 2.4: Types of beam-column joints in RC Structures 8
Figure 2.5: Types of load paths- Vertical loading and lateral loading due to earthquake 9
Figure 2.6: Failure of beam-column joint 10
Figure 2.7: Anchorage Failure Types of Hooked Bars 10
Figure 2.8: Bar terminator or mechanical anchor 12
Figure 2.9: Headed bar shown in red circle 12
Figure 2.10: Bearing forces in headed bar 13
Figure 2.11: Arrangement for pull-out test in shallow embedment 14
Figure 2.12: Head types 21
Figure 2.13: Load vs bar slip for monotonic pull-out tests for different head types 21
Figure 2.14: Clear distance between bars for different diameters 24
Figure 2.15: Headed bar with obstruction 24
Figure 2.16: Plan and elevation of headed bar embedded in concrete 26
Figure 2.17: Dimension measurement of centred embedded bar 27
Figure 2.18: Dimension measurement of side embedded headed bar 27
Figure 2.19: Location of headed bar 29
Figure 3.1: Ordinary Portland cement 43 grade 32
Figure 3.2: Sand after sieve analysis 34
Figure 3.3: Coarse aggregates - 12.5 mm down 36
Figure 3.4: Coarse aggregates - 20 mm down 36
Figure 3.5: Slump testing and cube casting process 37
Figure 3.6: Concrete cube specimen for compression testing 38
Figure 3.7: Concrete cube specimen during and after testing 38
Figure 3.8: Deformed bar of diameter 12 mm 39
Figure 4.1: Pull out test for longitudinal bars 40
Figure 4.2: Tetrahedron element 42
Figure 4.3: Stress-strain curve of reinforcement 44
Figure 4.4: Stress-strain curve in compression 45
Figure 4.5:Tension stiffening model 46

Figure 4.6: Validation of model when subjected to monotonic loading 50
Figure 4.7: Force vs Displacement for pull-out of reinforcement 50
Figure 4.8: Side split failure for lesser concrete cover 50
Figure 4.9: Plain head sample models 52
Figure 4.10: Grooved head sample models 52
Figure 4.11: Ribbed head sample models 53
Figure 4.12: Grooved Head dimensions 53
Figure 4.13: Ribbed Head dimensions 53
Figure 4.14: Headed bar 53
Figure 4.15: Cube with headed bar 55
Figure 5.1: (A) Fixing of cylindrical rod (B) Measurement by vernier calliper (C) Threading and making deformations (D) Finishing of threading 57
Figure 5.2: View of plain mechanical anchor fixed to rebar 57
Figure 5.3: View of Groove mechanical anchor fixed to rebar 57
Figure 5.4: View of Ribbed mechanical anchor fixed to rebar 58
Figure 5.5: Comparison of different mechanical anchors 58
Figure 5.6 Cone failure 59
Figure 5.7: Different type of plain headed main specimen (MS) 59
Figure 5.8: Different type of grooved headed MS 60
Figure 5.9: Different types of ribbed headed MS 60
Figure 5.10: Cube specimen without mechanical anchor 61
Figure 5.11: Curing of the specimen 61
Figure 5.12: Dimensions of upper plate and its oval shaped holes 62
Figure 5.13: Test setup with display unit 63
Figure 5.14: Test setup showing upper and lower plates fixed by bolting with UTM 63
Figure 5.15: Strain gauge at the surface of reinforcement bar near the top concrete surface end (SG1) 64
Figure 5.16: Strain gauge on the head surface (SG2) 64
Figure 5.17: Different type of headed bar used during experiment 65
Figure 5.18: System with data acquisition for strain recording 65
Figure 5.19: System connected with UTM 66
Figure 5.20: Fixing the specimen 66
Figure 6.1: Pull-out capacity of headed bar for different length of mechanical anchor for plain headed bar 69

Figure 6.2: Pull-out capacity of headed bar for different length of mechanical anchor for grooved headed bar 69
Figure 6.3: Pull-out capacity of headed bar for different length of mechanical anchor for ribbed headed bar 70
Figure 6.4: Effect of deformation over length for 11 mm length of mechanical anchor 70
Figure 6.5: Effect of deformation over length for 19 mm length of mechanical anchor 71
Figure 6.6: Effect of deformation over length for 27 mm length of mechanical anchor 71
Figure 6.7: Effect of deformation over length for 35 mm length of mechanical anchor 72
Figure 6.8: Effect of deformation over length for 43 mm length of mechanical anchor 72
Figure 6.9: Initial crack pattern near mechanical anchor 73
Figure 6.10: Final crack pattern at 60 mm displacement loading 74
Figure 6.11: Failure pattern 75
Figure 6.12: Bar and concrete specimen after failure 75
Figure 6.13: Comparison between pull-out capacity of different mechanical anchors 76
Figure 6.14: Stress-strain behaviour of G1L11 mechanical anchor 76
Figure 6.15: Failure pattern 77
Figure 6.16: Bar and concrete specimen after failure 77
Figure 6.17: Force vs Displacement curve for without anchor 78

LIST OF TABLES

Table 2.1: Relative head areas used in the previous studies 23
Table 3.1: Properties of cement as per IS 4031 33
Table 3.2: Sieve analysis of fine aggregates 33
Table 3.3: Sieve analysis of 12.5 mm down coarse aggregates 35
Table 3.4: Sieve analysis of 20 mm down coarse aggregates 35
Table 3.5: Mix proportion for M20 grade concrete per cubic meter 37
Table 4.1: Element types used 43
Table 4.2: Material properties for reinforcement bar 43
Table 4.3: Material properties for mechanical anchor 44
Table 4.4: Elastic properties of concrete 45
Table 4.5: Stress-strain behaviour of concrete in compression 47
Table 4.6: Stress-strain behaviour of concrete in tension 47
Table 4.7: Details of mechanical anchors and their sample notations 54
Table 5.1: Preliminary data used before testing 67

CHAPTER 1

INTRODUCTION

1.1 Backdrop

There has been huge population boom around many countries of the World, particularly in a developing country like India for the last two decades. In India alone, the decadal growth rate of population is around 17.70% (2011 Census of India). As per Government of India mission "Housing for All by 2022", 22 crores of residential buildings are to be constructed. Hence, rapid urbanization is required to meet the requirements of the growing population. However, the present towns, cities are already facing space constraints problems. Hence, to cop-up with the rapid urbanization and space constraints issues, there is a need of efficient and cost effective technologies of building construction. The present need of construction should take care of the following issues:

- Application of high amount of reinforcement which increases the amount of construction material leading to cost overrun.
- Availability of huge number of skilled and semi-skilled workers at site.
- Completion of construction projects within the scheduled time.

All the above mentioned issues sum up to increase the material, labour and operating cost with limited improvement in the construction progress. Hence, the overall scenario of construction industry, which depends mostly on technical design and site work, is incompetent due to the lack of efficient approach. Hence, to simplify and speed-up the construction practices, an effective and innovative technology should be introduced in construction industry.

1.2 Research significance

The dimensions of various members of reinforced concrete buildings (e.g. beams, columns, slabs, etc.) are finalized architecturally. Architects often prefer unique and irregular members in buildings with respect to simple and regular ones as a sign of distinctiveness. It is often observed that due to architectural beauty of the building, the member dimensions are being reduced. Beams and columns having smaller cross section are generally preferred in a reinforced concrete building. This makes the beam-column joint critical as it transfers both vertical and lateral loads from one member to another through a smaller volume. In this context, several factors come into play when the dimension of beam-column joint is reduced. Among

them, the high congestion of reinforcement with respect to the other portions of the member is a major problem as it leads to several problems. First, it may lead to honey-combing during concreting which reduces the strength of joint. Second, the bending of bars for adequate development length as per conventional methods seldom fits properly due to smaller dimension of the joint. Third, during the bending of the bar, the protective coating may crack which increases the chances of corrosion. With the present conventional methods, some of these problems can be solved by the inclusion of skilled workmen at site. But, it will increase the overhead cost and may also lead to increased completion time. The above mentioned problem can be reduced by using mechanical anchorage at beam-column joints. Hence, there is an immediate need for the development of an efficient and innovative mechanical anchorage mechanism to improve the performance of beam-column joints, especially when subjected to lateral loads.

1.3 Research objective

The present objective of the study is to understand behaviour of different mechanical anchor fixed at the end of the bar and embedded in concrete under tensile loading. Based on the literature review, design guidelines of the mechanical anchorage system are reviewed. It has been observed from the literature that very less information is available related to the length and deformations over the length of the mechanical anchor. Hence, looking at the research gaps in the literature and keeping the objective stated, the scope of the present research is limited to the development of an effective and innovative mechanical anchorage to provide adequate bond strength and to reduce the congestion of reinforcement at beam-column joint. For the purpose of achieving the goal, numerical and experimental studies of pull-out behaviour with different mechanical anchors is performed at the present study. The effective shape and size of the anchor is selected based on the pull-out testing. In the future study, that mechanical anchor will be used in the beam-column joint and compared with the performance of hooked bar used in the beam-column joint.

1.4 Research methodology

The present research is based on the numerical analysis in Abaqus and experimental studies of pull-out behaviour of reinforcement with mechanical anchor. Firstly, the numerical modeling is done to understand the pull-out behaviour with mechanical anchor. After that, the experimental investigations were being done. Based on the results of numerical and experimental investigations, conclusions are drawn and future scope of work are listed.

1.5 Organization of the thesis

The entire thesis is divided into eight different chapters. The first chapter includes the introduction part which reflects the backdrop, research significance, research objective and research methodology of the project. The second chapter includes extensive literature review of the past research works. It includes various numerical and experimental studies on the related topics. The third chapter includes the material characterization of the materials used. The fourth chapter includes numerical studies using non-linear finite element analysis (NEFA) in Abaqus. It deals with the pull-out behaviour of different mechanical anchorages. The fifth chapter covers the experimental investigation on different mechanical anchorages based on the pull-out behaviour of headed bars. The sixth chapter includes the results and discussions of the numerical and experimental studies. The seventh chapter comprises conclusions and future scope of work. Finally, in the eighth chapter, the references were being added.

CHAPTER 2

LITERATURE REVIEW

2.1 Bond and force transfer mechanism

Bond refers to the interaction between reinforced bar and concrete through which tensile load is transferred from steel into concrete (Thompson et al., 2002). When the bond stress of the bar is sufficient to resist the tensile load within the concrete, then the bar is developed and the embedment length necessary for the anchorage is called development/anchorage length (IS 456, 2000).

In any reinforced concrete construction, the force transfer mechanism from reinforcement to surrounding concrete is very important. In the deformed bar, these forces are transferred by the following ways (Figure 2.1):

- The chemical adhesion present between the concrete contact surface and reinforcing bar.
- The friction forces present due to bearing and shearing of the deformed bar and the chemical adhesion.
- Bearing and shearing forces due to the presence of ribs in the deformed bar.

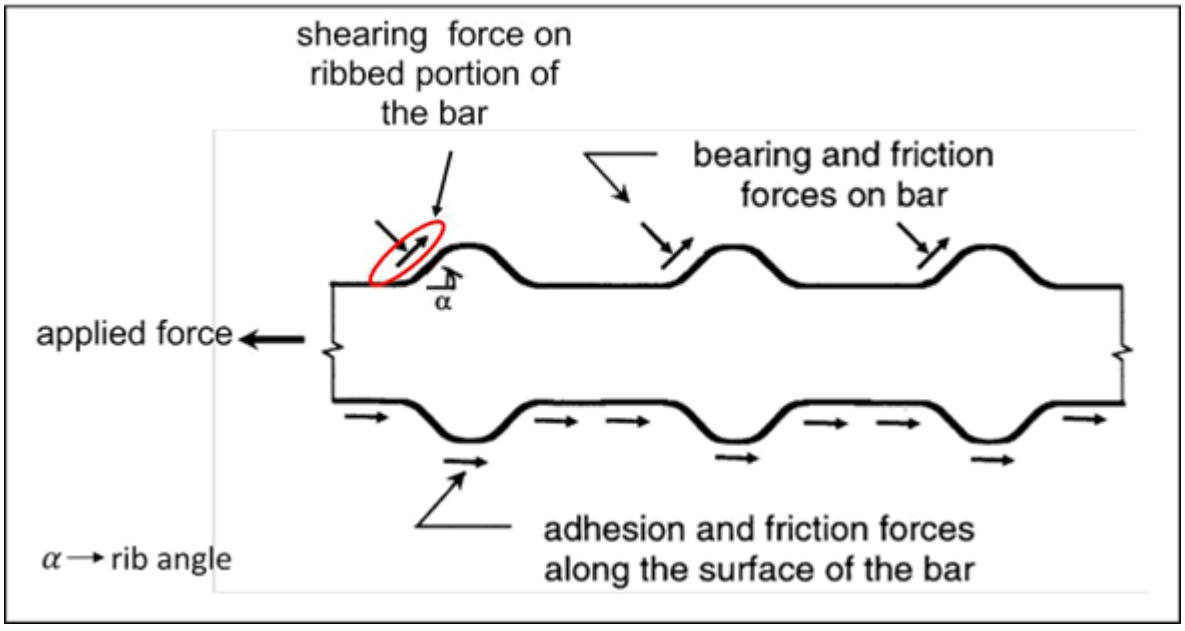

Figure 2.1: Different forces generated after applying external force (ACI Committee 408, 2003)

When tensile force exerts on the reinforcement bar having ribs, embedded in concrete, slip occurs in the bar. With slip, the adhesion force is lost and only bearing and friction forces are present. The component of compressive bearing forces normal to the surface of bar increase the value of friction forces. As slip increases, static friction forces decrease, leaving the forces at the contact faces between the ribs and the surrounding concrete. The forces are balanced by the shearing and bearing forces generated by the ribs present in deformed bars. These forces are resolved into tensile forces leading to generate cracking in the surrounding concrete which are both parallel and perpendicular to the direction. Conical wedges are formed when cracks generate in corners. Splitting crack can appear due to lack of concrete cover for transverse reinforcement. However, if the concrete cover, the spacing of the bar and the grade of concrete are sufficient, then pull-out failure occurs in which concrete shears in the direction of pull. **If the anchorage capacity of the reinforcing bar is sufficient then high stresses are generated in the bar so much so that the bar may reach to yield or even stress hardened zone (ACI 408R, 2003).** The force transfer mechanism is shown in Figure 2.2.

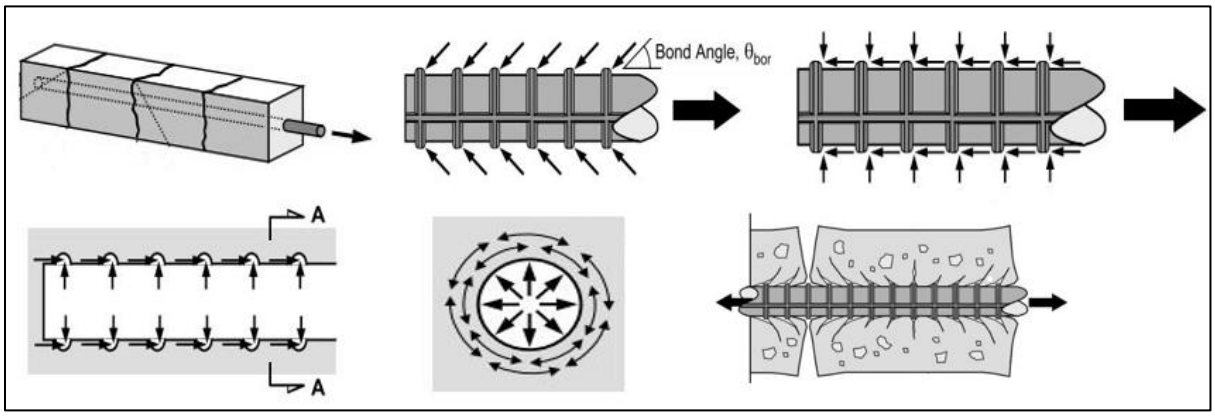

Figure 2.2: Force transfer mechanism (Goto et al., 1971)

The bond force-slip response of reinforcing bars is the function of the relative rib area (defined as the ratio of bearing area of bar deformations to the shearing area between the deformation) of the bars. Under all conditions of bar confinement, the initial stiffness of load-slip curves increases with an increase in the relative rib area. Under conditions of relatively low confinement, in which bond strength is governed by splitting of the concrete, bond strength is independent of the deformation pattern. Under conditions in which additional bar confinement is provided by transverse reinforcement or higher cover, bond strength increases compared to the bond strength of bars with less confinement. The magnitude of the increase in bond strength increases with an increase in the relative rib area (Darwin et al., 1993).

2.2 Development length formulation

The development length is the embedment length of reinforcement necessary within the concrete to develop sufficient bond strength for resisting the applied tensile force (Figure 2.3).

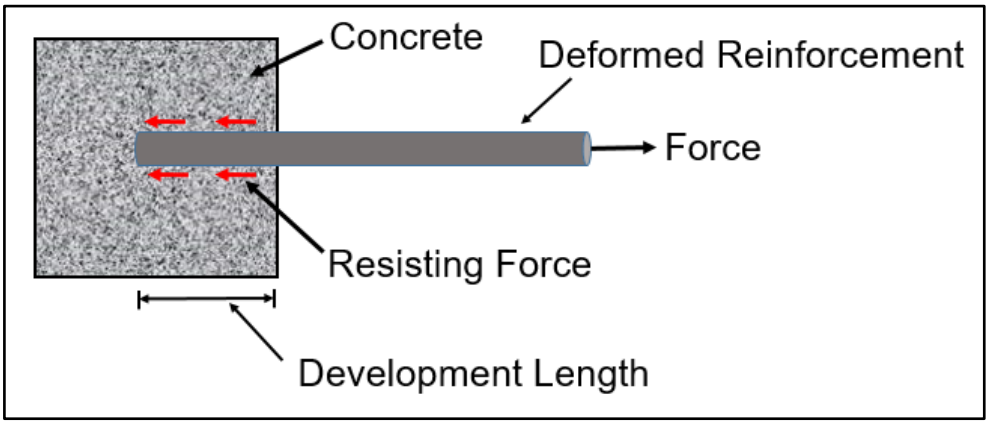

Figure 2.3: Schematic view showing development length of bar in concrete

Development length provision as different codal provisions are as follows:

2.2.1 Indian Standards

Development length formula for plain bar in tension is given as (IS 456: 2000):

$$L_d = \frac{\emptyset \sigma_{st}}{4\tau_{bd}} \qquad \text{Eqn. 2.1}$$

Where,

$\emptyset$ = nominal diameter of the bar (mm)

σ_{st} = stress in bar at the section considered at design

τ_{bd} = design bond stress (MPa) for plain bar in tension

d_b = diameter of the bar (mm)

For deformed bars the value of design bond strength is increased by 60% and for bar in compression its value is increased by 25%. The value of development length needs to be increased by $4d_b$ for every 45^0 bend; subjected to a maximum of $16d_b$ for a standard U-type hook. The value of development length given in IS 456: 2000 which considers static loading condition. When the dynamic load like earthquake is considered then the anchorage length can be calculated according to the provision of IS 13920: 2016. Its value is taken as:

$$L'_d = L_d + 10d_b \qquad \text{Eqn. 2.2}$$

The formula given as per Indian Standards has not considered the effect of epoxy coating and lightweight concrete, if any.

2.2.2 ACI Standards

The formula of development length for deformed bar or deformed wire is given as (ACI 318: 2011, Section 12.2.3):

$$K_{tr} = \frac{40 A_{tr}}{sn} \qquad \text{Eqn. 2.3}$$

$$L_d = \frac{3}{40} \frac{f_y}{\lambda \sqrt{f'_c}} \frac{\Psi_t \Psi_e \Psi_s}{\frac{c_b + K_{tr}}{d_b}} d_b \qquad \text{Eqn. 2.4}$$

$$\frac{c_b + K_{tr}}{d_b} \leq 2.5 \qquad \text{Eqn. 2.5}$$

where,

λ = a factor that depends on concrete type (for lightweight $\lambda = 0.75$; normal weight $\lambda = 1.0$)

Ψ_t = casting position factor

Ψ_e = a factor that depends on coating

Ψ_s = a factor that depends on size of the bar used

c_b = smaller of: (a) the distance from centre of a bar or wire to nearest concrete surface, and (b) one-half of the centre to centre spacing of bars or wires being developed (in.)

s = centre to centre spacing of transverse reinforcement (in.)

A_{tr} = total cross-sectional area of all transverse reinforcement within spacing s that crosses the potential plane of splitting through the reinforcement being developed, ($in.^2$)

n = total number of transverse reinforcement

d_b = diameter of bar (in.)

2.3 Beam column joint

2.3.1 General

A beam–column joint is that portion of column within the depth of deepest beam that frames into the column. A connection is the joint plus the columns, beams, and slab adjacent to the joint. Typical cast-in-place reinforced concrete beam-column joints are shown in Figure 2.4. The connection of the beam to the beam-column joint region may be in the two different

directions. The beam for which joint shear is considered is called longitudinal beam while the beam in perpendicular direction of longitudinal beam is known as transverse beam. Three types of beam-column joints are considered as follows (ACI 352R, 2002):

- Interior Joint
- Exterior Joint
- Corner (Knee) Joint

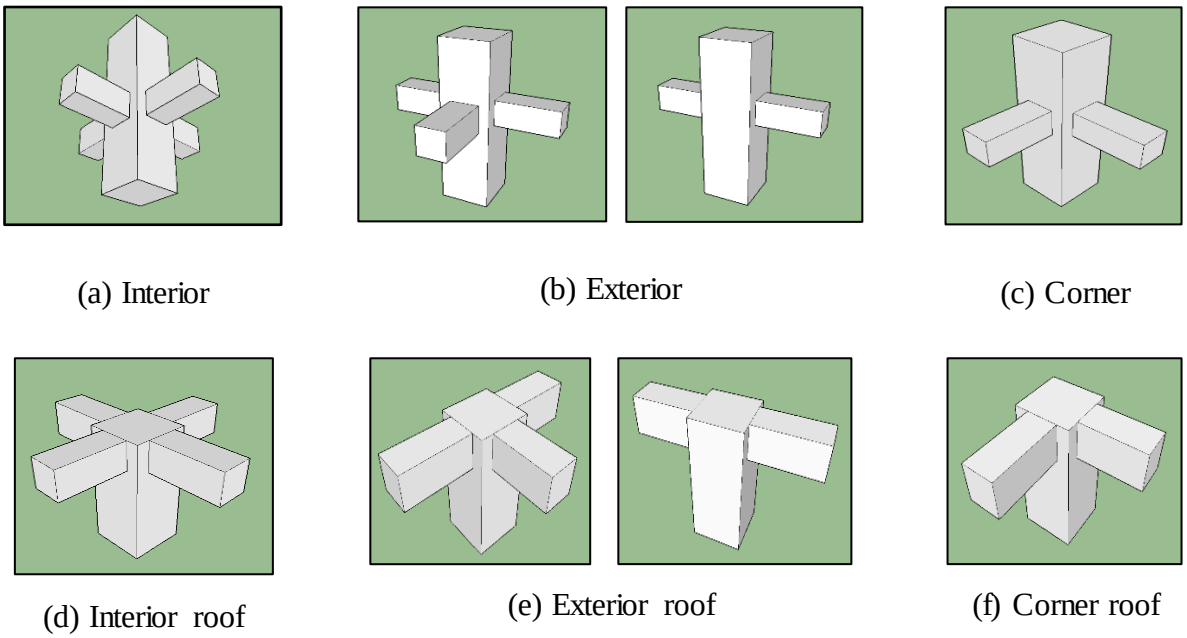

(a) Interior (b) Exterior (c) Corner

(d) Interior roof (e) Exterior roof (f) Corner roof

Figure 2.4: Types of beam-column joints in RC structures (ACI 352R, 2002)

Based on loading conditions and estimated deformations while resisting lateral loads, beam-column connections are classified into two types as follows (ACI 352R, 2002):

- Type-I Connection: It is the connection composed of members which is designed with no consideration of significant inelastic deformation.
- Type-II Connection: It is the connection in which frame members are designed to have sustained strength under deformation reversals into the inelastic range.

In other words, Type-I connection is the moment resisting connection and designed based on strength whereas Type-II connection are having member to dissipate energy through reversal of deformation in inelastic range. Two types of load paths are considered - Vertical load path and Lateral load path. The vertical load path is generally due to the gravity load which is static in nature. The load transfers from the slab to the beam, then beam to column through beam-

column joint columns, column to foundation and finally to the subsoil. In the lateral load case, only seismic loading is considered. The load path is shown in Figure 2.5.

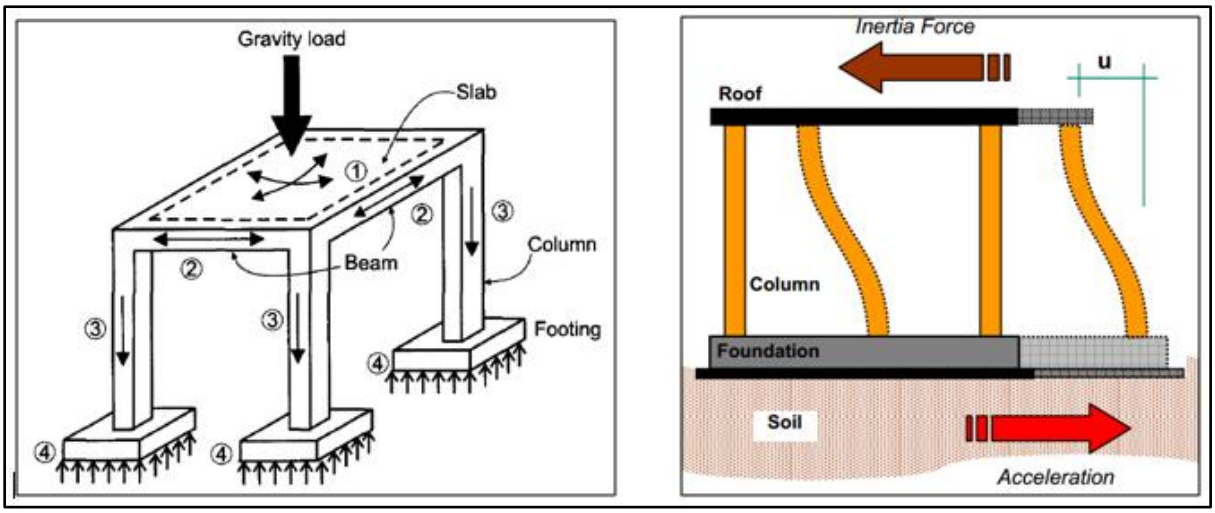

Figure 2.5: Types of load paths- vertical loading and lateral loading due to earthquake (Murty, 2005)

A typical beam-column joint failure is shown in Figure 2.6. In the beam-column joints, generally two types of failure are predominant (Goto et al., 2012):

- Shear failure: It occurs due to the excessive shear force and inadequate development length of beam bars in the joint. It is difficult to curb as reinforcement bars developed are complicated at the joint due to presence of transverse reinforcement.
- Slip/Anchorage failure: It occurs due to presence of shorter development length in addition to shear failure.

All types of anchorage failures are caused by large compressive stress generated inside of bent portion. There are three types of anchorage failure which is as follow (Goto et al., 2012):

- Side split failure: It occurs due to less thickness of concrete cover. In this case, concrete located at the adjacent side of bent portion of joint is fractured in split (Figure 2.7(A)).
- Local compressive failure: In this case, fracture of concrete occurs due to bearing stress inside the bent portion of joint. It happens due to less radius of bend bar (Figure 2.7(B)).
- Raking failure: In this case, concrete in the front portion of joint is raked out as a single body due to poor concrete or lesser development length (Figure 2.7(C)).

Figure 2.6: Failure of beam-column joint (Sengupta et al., 2013)

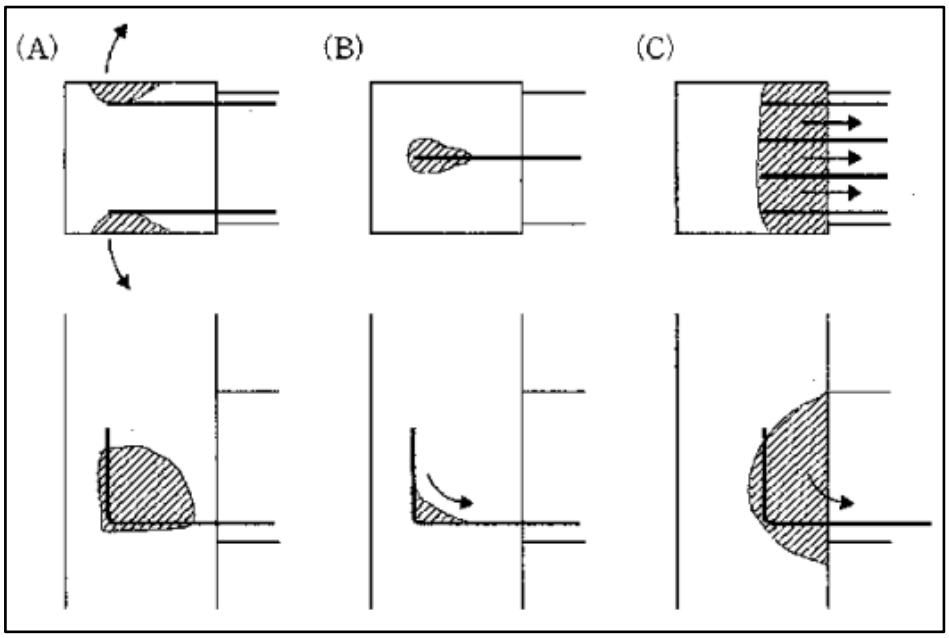

Figure 2.7: Anchorage failure types of hooked bars (Goto et al., 2012)

As per research methodology, both the conventional hooked bar anchorage and headed bar anchorage can be used in beam-column joints. But, the headed bar anchorages are more efficient than hooked bar anchorages. In hooked bar anchorage, longer development length is required, while, in by using headed bar, hooks are eliminated and the development length reduces significantly.

2.4 Design considerations for beam-column joint

2.4.1 General

In general, the design considerations for a mechanical anchorage are as follows:

- The connection should be designed for the most critical combination of forces.
- The connection should be strong enough to resist the load which will be transferred to the adjacent members.
- The forces (and moments) considered at these connections are axial forces, shear forces, lateral forces, bending moment and torsion.
- Final approval by engineer-in-charge or building official is a must.

2.4.2 Conventional Methods

In this method, for the anchorage at the beam-column joints, the reinforcement used is bent in 90^o or 180^o hook which is developed either within the beam or column. In the present scenario, most of the construction practices use this method. The strength of the anchorage is determined by pull-out test, cyclic loading test or beam end test of the beam specimen. The explanation of the bends and hooked bars are described in the Indian Standards as well as in the other standards (IS 456: 2000; ACI 318: 2011). In this method, the congestion of reinforcement at the joint occurs. During earthquake, significant shear force is generated at the beam column joint, to withstand this shear force large development length is required leads to congestion of reinforcement and honey-combing for which enlarged L_d is to be provided. Due to the lack of development length, the anchorage failure occurs along with the shear failure (Goto et al., 2012), which have commonly been observed in RC-MRF structures during post-earthquake survey.

2.4.3 Mechanical anchors

Use of mechanical anchors are the alternative of the conventional method of anchorage. Efforts are made to use it in the beam-column joint region. A mechanical anchor is shown in Figure 2.8 and its use in beam-column joint is shown in Figure 2.9.

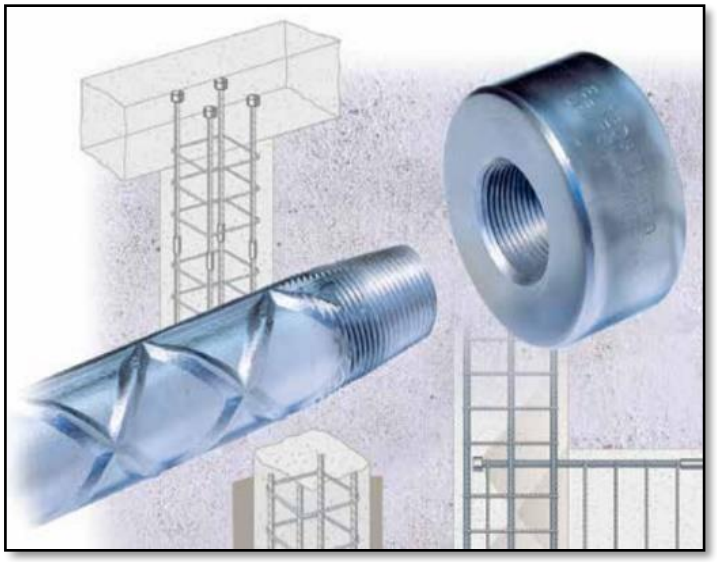

Figure 2.8: Bar terminator or mechanical anchor (Pentair, 2017)

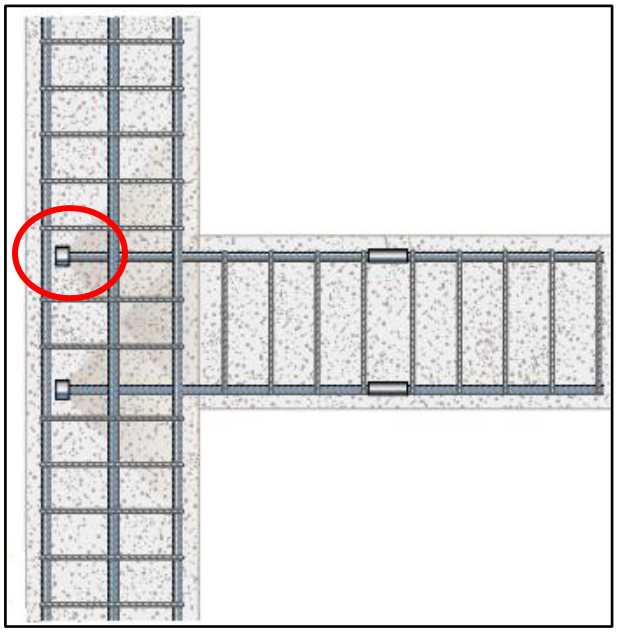

Figure 2.9: Headed bar shown in red circle (Pentair, 2017)

2.5 Headed bars

2.5.1 Background

The force transfer in the headed bar is due to the bearing of the deformation in the bar as well as the bearing of head. However, the major forces are transferred due to the bearing of the head. Resisting forces in the headed bar are shown in Figure 2.10.

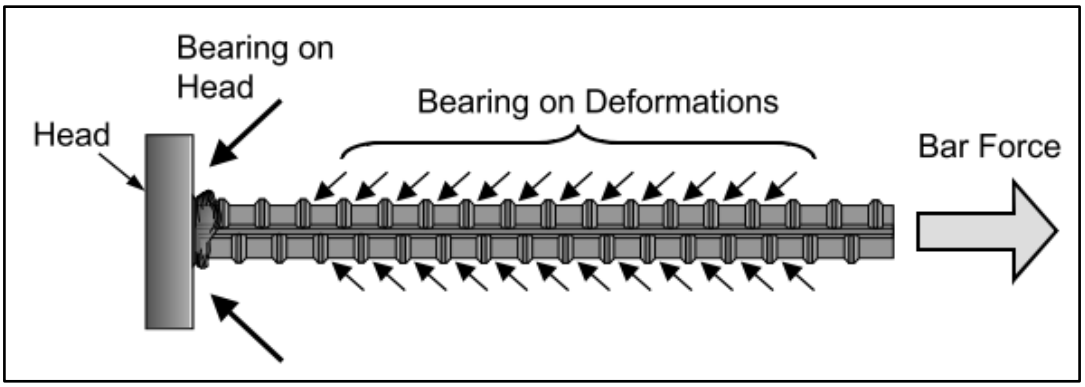

Figure 2.10: Bearing forces in headed bar (Thompson et al., 2002)

The development of a headed bar in the beam-column joint was started from its use as the headed stud anchors. The headed stud anchors were used to provide the anchorage between the steel girders and the deck slabs. Some of the work had been done in the Lehigh University (McMackin et al., 1973). Further its use was increased in the flat slab as the punching shear reinforcement (Digler et al., 1981; Mokhtar et al., 1985). The shear reinforcement provided in the slab was used with very small closed loop which was very difficult to create. An effort was made to use double headed stud as an alternative for the shear stirrup provided in the slab (Digler et al., 1981; Mokhtar et al., 1985). Different shapes like I-section, bar with square plate attached on both ends etc. were tried. Later, the use of headed bar was further increased as an alternative method of anchorage in bridge structures (Stoker et al., 1974). The main purpose of the study was relevant to reduce the congestion created due to large amount of hooked bar and to reduce the required development length. In 1980's, the Alaska Oil and Gas Association (AOGA) studied the use of double headed stud for the shear reinforcement to construct a concrete platform. Further, the use of headed bar in the disturbed region was observed by Berner and Hoff, 1994.

2.5.2 Previous research

2.5.2.1 University of Texas

At the University of Texas most of the previous research work was carried out by DeVries, 1996 and Bashandy, 1996. DeVries, 1996 conducted pull out test with headed bar to find the variables on which the pull-out capacity depends. Based on this test, some relations with the variables were formulated for anchorage capacity. During the experiments, over 160 pull out test were conducted to understand the effect of different variables. The whole tests were divided in two phases, one in shallow embedment while the other in deep embedment. Shallow and deep embedment were chosen based on the ratio of embedment depth to clear concrete cover.

The ratio of less than 5 was described as shallow embedment whereas ratio greater than 5 was defined as deep embedment. The main variables considered in the study was compressive strength of concrete, edge distance, embedment depth, head size, development length and the effect of transverse reinforcement. The different notation is shown in Figure 2.11. For shallow embedment, the concrete breakout capacities were formulated as:

$$N_n = \frac{A_n}{A_{No}} \Psi_1 N_b \qquad \text{Eqn. 2.6}$$

$$N_b = 22.5(h_d)^{1.5}\sqrt{f'_c} \qquad \text{Eqn. 2.7}$$

$$\Psi_1 = 0.7 + 0.3\frac{c_{min}}{1.5h_d} \leq 1 \qquad \text{Eqn. 2.8}$$

Where,

N_b = the basic concrete breakout capacity (lbs)
Ψ_1 = modification factor for stress disturbance
A_n = projected area of concrete breakout failure (in.^{2})
h_d = embedment depth (in.)
A_{No} = basic projected area of a single anchored bar, 9(hd^2) (in.^{2})
c_{min} = minimum edge distance (in.)
$f_{c'}$ = concrete compressive strength (psi)

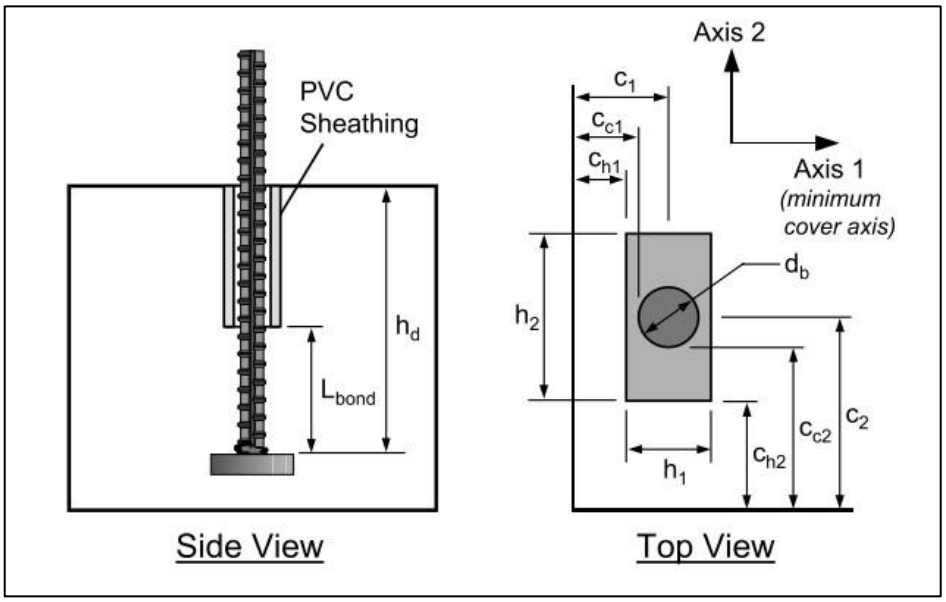

Figure 2.11: Arrangement for pull-out test in shallow embedment (Thompson et al., 2002)

In the deep embedment test, the variables considered were head orientation, head shape, size and thickness, development length, embedment length, concrete compressive strength, clear concrete cover, placement of reinforcement bar, and transverse reinforcement. For the deep embedment side blow out capacity were formulated:

$$N_n = \frac{A_{Nsb}}{A_{Nsbo}} \Psi_2 N_{sb} \quad \text{Eqn. 2.9}$$

$$N_{sb} = 144 c_1 \sqrt{A_{nh} f'_c} \quad \text{Eqn. 2.10}$$

$$\Psi_2 = 0.7 + 0.3 \frac{c_2}{3c_1} \leq 1 \quad \text{Eqn. 2.11}$$

where,

N_{sb} = the basic side blow-out capacity (lbs)
Ψ_2 = modification factor for stress disturbance caused corner affects
A_{Nsbo} = basic projected side blow-out area of a single anchored bar ($in.^2$)
A_{Nsb} = projected area of side blow-out failure ($in.^2$)
c_1, c_2 = the minimum and maximum edge distances (in.)

The following conclusions can be drawn:

- In shallow embedment, the failure was due to pull out cone failure whereas in the deep embedment, the failure was due to side blow out failure or bar fracture.
- No visible effects were found due to the orientation of head, aspect ratio for rectangular head and due to head shape.
- No effects were found on the ultimate capacity due to the transverse reinforcement.
- With the increase in head size, the side blow out capacity increased.
- The ultimate capacity increased with grade of concrete.
- The bonding due to the bar attached with head increases the ultimate capacity and improves the slip of the bar.
- The ultimate capacity increased with the distance of head from the edge.
- At failure, it was found that approximately one-third load was resisted by development length and the remaining was resisted by the head. But, this conclusion was based on a very limited experimental result.

Bashandy et al., 1996 conducted experiment to find out the possibility of headed bar to use as a transverse reinforcement. In the other part of the study, the effect of cyclic loading was also considered. The results of the experiment showed that the cyclic loading between 5 to 80% of the ultimate capacity up to 15 cycles did not show any noticeable effect on the anchorage capacity. Blow out capacity increased with the crossing bar in the head anchorage zone. But it is not effective for small head with large cross sectional area of the crossing bar. A total of 32 beam-column joint specimen were tested in which beams were not casted but simulated with tensile forces to find out the effects of relative head area, head aspect ratio, head orientation, concrete compressive strength, bar diameter, and embedment depth. During testing, most of the specimen failed in side blow out failure while some specimen failed in shear. In the side blow out failure, the longitudinal crack appeared at the face of the column and it propagated radially along the embedment length and finally concrete cover spelled out whereas in shear failure the failure occurred due to the increased crack width without spalling of concrete cover.

The following conclusions can be drawn from the above study:

- There were no noticeable effect of head orientation and aspect ratio which was similar with conclusion drawn by DeVries et al., 1996.
- With the increased embedment length, the ultimate capacity increased.
- The transverse reinforcement which were placed parallel to the axis of the headed bar restrained the side cover from blow out.
- The capacity found by deep embedment test was less about 14 to 44 % than found by DeVries et al., 1996. It was due to the reason that the head used by Bashandy et al., 1996 was smaller than used by DeVries et al., 1996.

2.5.2.2 Kansas University

The study on headed bars were conducted by J. L. Wright and S. L. McCabe in 1997. 70 beam end specimens were tested to find out the formula for the development length of headed bar. In the specimen, the bar used were hooked with 180^0 bent, headed bars or non-headed bars. The headed bar used were friction welded type. The study parameters were clear concrete cover, compressive strength of concrete and the arrangement of transverse reinforcement.

The following conclusions were drawn from the experiments:

- The load carried by using headed bar were equal or even better than the hooked bar during the test.
- When the amount of confining reinforcement was increased then the increased concrete cover on failure load had no effect. Hence, there is no need to provide both large amount of cover with large amount of transverse reinforcement.
- Up to 50% capacity was increased with the increase of transverse reinforcement. After that, with further increase, the failure capacity got reduced.

The formulation for the development length of headed bar were given as:

$$\boldsymbol{L_{dt}} = \frac{\boldsymbol{22 d_b f_y}}{\boldsymbol{60\sqrt{f'_c}}}\left(\frac{\boldsymbol{3 d_b}}{\boldsymbol{c+K_{tr}}}\right)(\boldsymbol{\alpha\beta\lambda\Psi}) \geq \text{maximum of } (6d_b \text{ or } 152.4 \text{ mm}) \qquad \text{Eqn. 2.12}$$

$$\frac{\boldsymbol{c+K_{tr}}}{\boldsymbol{d_b}} \leq \boldsymbol{2.5} \qquad \text{Eqn. 2.13}$$

$$\boldsymbol{K_{tr}} = \frac{\boldsymbol{A_{tr} f_{yt}}}{\boldsymbol{1500 sn}} \qquad \text{Eqn. 2.14}$$

The minimum three transverse reinforcements were recommended and its amount should be:

$$\boldsymbol{A_{tr} f_{yt}} \geq \text{maximum of } (2000\text{lb/in};\ 5d_b) \qquad \text{Eqn. 2.15}$$

where,

d_b = diameter of the bar (in.)

f_y = yield strength of the bar (ksi)

f'_c = compressive strength of concrete (ksi)

c = minimum cover of the bar (in) $\geq 3d_b$

A_{tr} = total area of transverse reinforcement within the spacing (s) that crosses the plane of splitting through the reinforcement being developed ($in.^2$)

f_{yt} = yield strength of transverse reinforcement (psi)

α = casting position factor

β = epoxy-coated reinforcement factor

λ = lightweight aggregate factor

Ψ = excess reinforcement factor

The value of α, β, λ and Ψ did not determine on that time and it needs furthermore research to determine these factors.

2.5.2.3 Other studies

Wallace et al., 1998 tested two corner and five inter-story exterior beam-column joint. The beam-column joints were constructed by using hooked bars (conventional method) as well as headed bars. Cyclic loading test were performed with 4 to 6% drift ratio and the performance of the joints with hooked bar and headed bar were compared. The test results showed that the performance of inter-story exterior joints with headed bar was better as compared to the hooked bar. The results with the corner joints with no transverse beam, the joint shear stress level was limited. At higher shear level, the flexural capacity did not reach and a significant joint deterioration was observed. With the headed bar, beam and column reinforcement cage can be constructed separately.

Park et al., 2003 studied the effect of head plate shape and thickness of headed bar. The headed bar used was of welded type. Pull out test were conducted and the types of failure were predicted as pull concrete break out failure, reinforcing bar failure, or pull through failure. The variables were bar size, head shape, dimension of head plate and type of welding. The variables like concrete strength and embedment depth were also considered. The embedment depth was taken as 70 mm for shallow embedment and 100 mm for deep embedment. Based on the experimental studies, it can be concluded that with increase of thickness, the anchorage capacity increases keeping the diameter of the head to be constant and shape is circular. The anchorage capacity also increases with the increase of diameter of head. In shallow embedment, the failure takes place as concrete break out failure having anchorage capacity less than pull through failure and reinforcing bar failure in circular head.

After DeVries et al., 1996; Bashandy et al., 1996 and Wright et al., 1997, Thompson et al. 2006 developed a model to predict the anchorage capacity of the headed bar. The total anchorage capacity of the headed bar is provided by the head bearing and the bonding mechanism. Separate equations for both head bearing capacity and bond are formulated.

The formula for bar stress at head is given as:

$$\boldsymbol{f_{s,head} = n_{5\%} \times 2 \times f'_c \times \frac{c}{d_b} \times \sqrt{\frac{A_{nh}}{A_b}} \times \Psi} \qquad \text{Eqn. 2.16}$$

$$\boldsymbol{\Psi = 0.6 + 0.4 \times \left(\frac{c_2}{c}\right) \leq 2.0}$$ Eqn. 2.17

The formula for bond stress is given as:

$$\boldsymbol{f_{s,bond} = \chi.\left(\frac{L_a}{L_d}\right).f_y}$$ Eqn. 2.18

$$\boldsymbol{\chi = 1 - 0.7\left(\frac{1}{5}\frac{A_{nh}}{A_b}\right) \geq 0.3}$$ Eqn. 2.19

where,

$f_{s,\ head}$ = bar stress (N/mm^2)

N = normal force (N)

A_{nh} = effective head area (mm^2)

$n_{5\%}$ = 0.7 recommended, to adjust the model such that the only 5% of the result are having the capacity less than calculated by the model.

f'_c = concrete compressive strength from cylinder test (N/mm^2)

c = minimum cover dimension (mm), taken from the centre of the bar

A_b = area of reinforcement (mm^2)

c_2 = minimum cover dimension in the direction of perpendicular to (c) (mm)

d_b = diameter of reinforcement (mm)

L_a = anchorage length (mm)

L_d = development length (mm)

χ = reduction factor

The given model is only valid for concrete compressive strength greater of equal to 28 MPa and the anchorage length greater than or equal to $6d_b$.

Another model was developed by Hong et al., 2007 to find out the anchorage capacity and bonded length of headed bar. Later on, it was found by Chun et al., 2009 that existing model of Thompson et al., 2006 do not properly predict the concrete contribution to anchorage strength of headed bars terminated in exterior joints. A new model was proposed that accounts for head bearing and bond capacity of the anchored bars.

The formula for head bearing is given as:

$$P_{head} = [1 + 2.27(l_e - 0.7D_c)/D_c]0.85f'_cA_{nh}$$

Eqn. 2.20

The formula for bond capacity of headed bar is given as:

$$P_{bond} = 0.504\sqrt{f'_c}\emptyset_b(l_e - d_b) \quad \text{Eqn. 2.21}$$

where,

l_e = embedment length (mm)
D_c = column depth (mm)
$\emptyset_b$ = perimeter of bar (mm)
A_{nh} = effective head area (mm^2)
f'_c = concrete compressive strength from cylinder test (N/mm^2)
d_b = diameter of bar (mm)

An improved model was developed by Caldentey et al., 2013 for the capacity of concrete to carry out the concentrated load. When it was compared with the experimental results as well as the other existing models then it was found to be more improved. Similarly, plate-anchored reinforcement bars can be used in buildings, overpass or underpass for faster and improved construction details as well as to make it more flexible and economical. Eurocode does not specify any specific codal provisions for plate anchorage. ACI provides empirical formula for the plate-anchored reinforcement bars which are based on types of failure (comparatively smaller plate size gives compression failure and larger plate size gives side-blowout failure).

Rajagopal et al., 2014 studied the nonlinear finite element analysis with hooked and headed bar. The flexural strength capacity of the plate-anchored system at knee-joint i.e. corner joint is the minimum of the proposed formulas by ACI as per failure (Marchetto et al., 2016).

2.5.3 Factors affecting anchorage capacity of headed bars

The factors on which the anchorage capacities of headed bars depend are as follows:

- Head attaching techniques
- Loading conditions
- Head geometry (includes head shape, head size, head thickness and orientation of the head)
- Clear concrete cover of the bar

- Clear distance between two bars
- Embedment depth

2.5.3.1 Head attaching techniques

Head can be attached either by welding, threading or by forging. The attached head should fulfil the requirement of ASTM A970/A970M, 2016 standard. Kang et al., 2010 found that the head attaching techniques - welded versus threaded had negligible influence on the anchorage capacity for small headed bars (refer Figure 2.12 and 2.13).

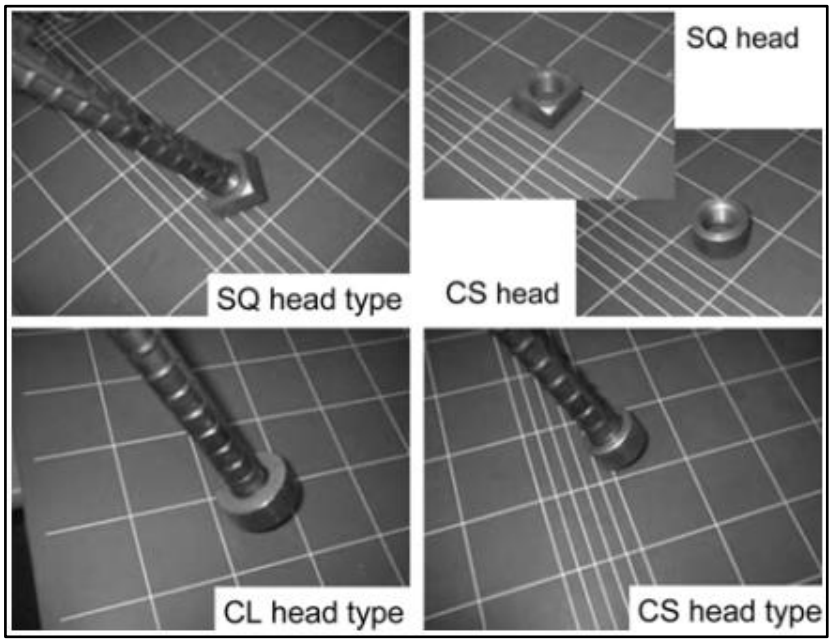

Figure 2.12: Head types (Kang et al., 2010)

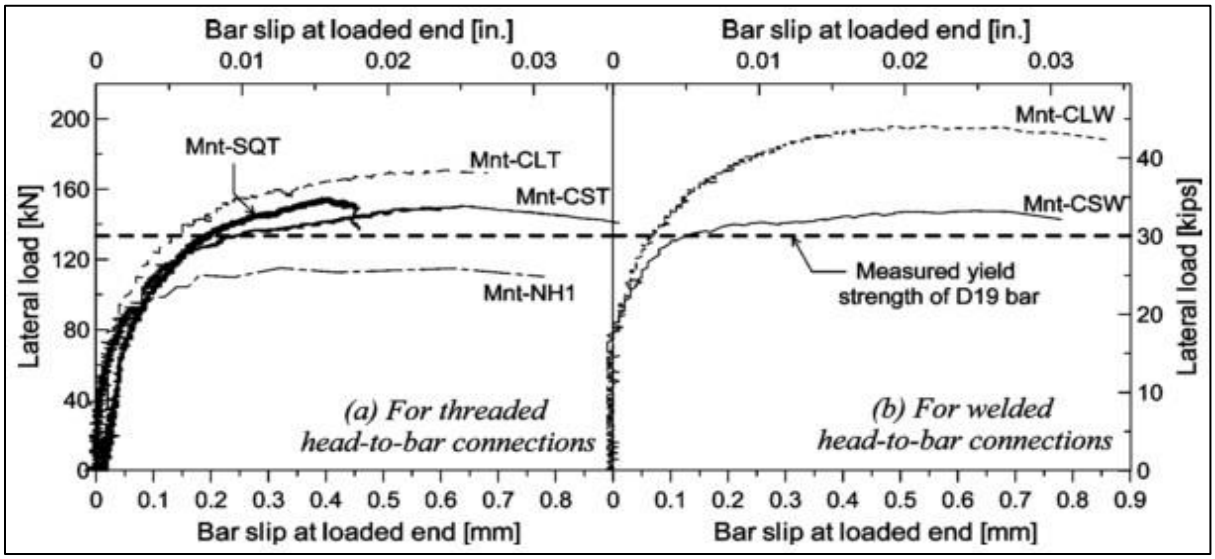

Figure 2.13: Load vs bar slip for monotonic pull-out tests for different head types - SQ is square; CL is circular large; CS is circular small; NH is no head (Kang et al., 2010)

2.5.3.2 Loading conditions

Kang et al., 2010 showed that the effect of loading monotonic vs repeated has no visible effect on small headed bar. Most of the test were done on cyclic loading test and no such comparison was made. Although for the large headed bar, results may vary.

2.5.3.3 Head geometry

Head geometry includes head shape, head size, head thickness and orientation of the head.

The previous studies have been done on the square, circular, rectangular and elliptical shape of a head plate. DeVries, 1996 used the square and rectangular shape of different dimension and conducted pull out the test. The result was indicated that there was not much influence of the head shape on the ultimate capacity when compared with rectangular and square shape head. Also it was found that the aspect ratio and the orientation of rectangular type head did not have much influence. Another experiment conducted by Bashandy, 1996 and Kang et al., 2010 showed the same result on circular versus square shape head. Park et al., 2003 conducted an experiment with the various type of plate shape. The plate shape was circular, square, rectangular and elliptical. It was concluded that there was some effect of shape on anchorage capacity. Numerically, it was not clearly predicted due to limited experimental data and a lot of variables.

One of the main variables for the headed bar is the relative head area. The relative head area is defined as the ratio of head area minus the area of the bar to the area of the bar in the head having no sleeve connection. If the head is attached with a sleeve connection then the relative head area is defined as the head area minus the area of obstruction to the area of the bar (ACI 318, 2011). With the increase of the relative head area, the anchorage capacity increases (Kang et al., 2010). The required anchorage capacity is mainly obtained by the development length provided and the bearing of the head (Kang et al., 2009). According to ACI 318, 2011, there should be $4d_b$ (where d_b is the diameter of the bar) clear spacing between the beam bars from which the head is attached. With the increase of relative head area, the size of the head increases which again creates a problem regarding the limitation of the clear bar spacing as the cross-section of the beam and column are limited. Although, there is a provision in ACI 318, 2011 to put the headed bar in staggered form. But with the large increase of the head, again the congestion occurs and also the ACI 318, 2011 provision related to bar clear spacing do not fulfil. Park et al., 2003 tested different type and found there is some degree of effect but it did not exactly quantify the effect of each particular variable. Kang et al., 2010 found that the small

relative head area approximately 2.6 can also be used. Table 2.1 shows the relative head area used in the previous studied.

Table 2.1: Relative head areas used in the previous studies

Authors	Relative head area $(A_{head}- A_b)/A_b$
Wallace et al., 1998	4
DeVries et al., 1999	5-10
Park et al., 2003	5-14
Chun et al., 2007	3-4
Lee et al., 2009	5.3
Kang et al., 2010	2.6-4.9
Kang et al., 2012	5.4
Dhake et al., 2015	4

2.5.3.4 Clear concrete cover

Clear concrete cover is one of the main parameters which decides the failure criteria of the pull-out behaviour of the headed bar. In case of lesser concrete cover, blow out failure occurs before the reinforcing bar failure or pull through failure in the pull-out test. As a result, lower failure capacity was recorded. Research was conducted for minimum clear bar spacing so that the actual capacity of the headed bar can be explored. ACI 318, 2014 provides a minimum clear concrete cover of 38 mm for the protection of reinforcement in concrete and for headed bar, minimum $2d_b$ is recommended to prevent blow out failure. In both of the criteria, higher value is adopted during the design.

2.5.3.5 Clear distance between two bars

The clear distance between two adjacent headed bars is different for different diameter of bars. As per Kang et al., 2009, the ratio of bar clear spacing to diameter of the bar ranges between 1 to 5. The values of the ratio are randomly spaced for different diameters. ACI 318, 2014

recommends that the minimum bar clear spacing should be 4 times the bar diameter. The clear spacing between bars used by the previous researchers are shown in Figure 2.14.

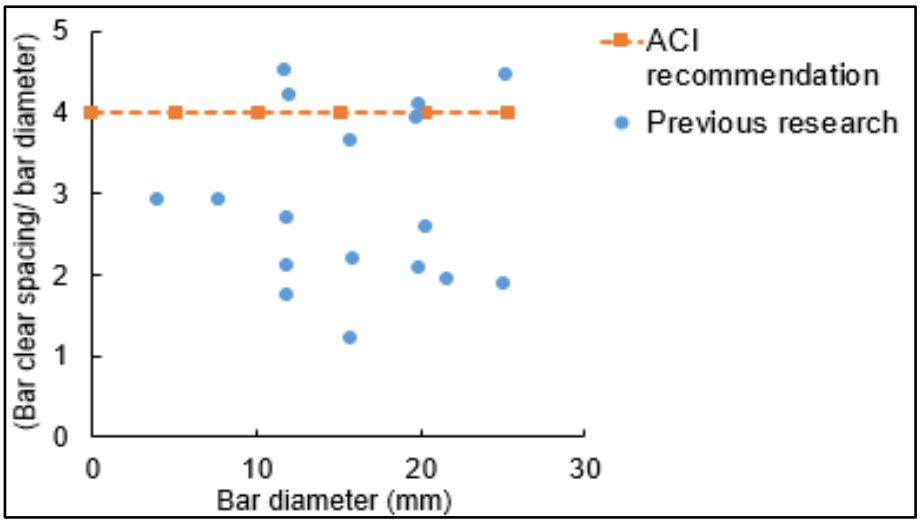

Figure 2.14: Clear distance between bars for different diameters (Kang et al., 2009)

2.5.3.6 Embedment depth and development length

Embedment depth and development length are the most important parameters which decide the failure type and capacity. Embedment length can be defined as the distance between the surface of the loaded specimen and nearer surface of the head plate (DeVries et al., 1996). The development length for the headed bar is defined as the distance from the deformed bar attached from the head to a critical section (DeVries et al., 1996). It was found that with the increase of embedment length, the failure pattern changes. For the deep embedment, side blow out failure or bar fracture failure occurs while in shallow embedment pull cone failure occur as explained earlier (DeVries et al., 1996).

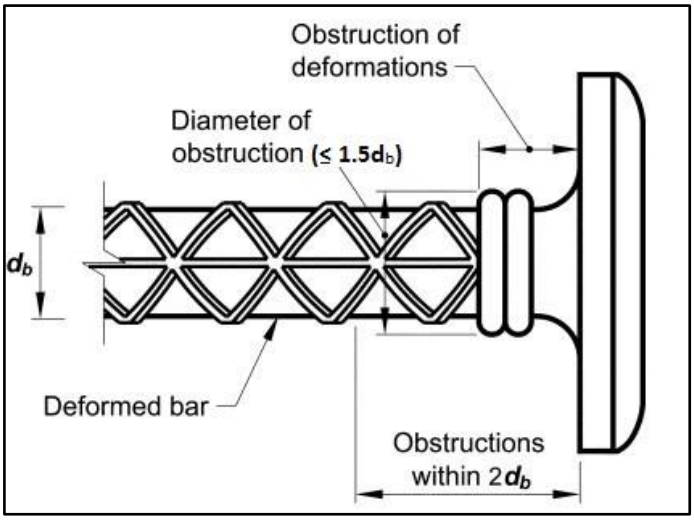

Figure 2.15: Headed bar with obstruction (ACI 318, 2011)

2.5.4 Summary of codal provisions

2.5.4.1 ASTM A970/A970M, 2016

This codal provision explains about the head attaching techniques and the minimum strength of the head so that it does not fail during the application of load. The head can be either attached by welding or threading. The threaded head can be used by two ways: First, the thread can be made in the head as well as at the end of the deformed bar and both are put together. Second, the head is having a non-threaded hole and it is fit in the deformed bar and tight it through the nut. It is explained that the headed bar can provide sufficient anchorage if it is detailed properly. The provided head and bar connection should be strong so that the failure does not occur due to the connection failure of parent head and the bar. The headed bar can be classified as Class A headed bar and Class B headed bar. Class A headed bar is designed to resist minimum tensile stress whereas Class B headed bar is designed to resist minimum tensile stress as well as specified elongation. For the headed bar, two basic test tensile and bend test are needed to ensure the proper attachment of the head with the parent bar. For the threaded head, bend test is not required.

2.5.4.2 ACI 318, 2014

As per ACI 318, 2011, some of the guidelines related to headed bar are explained below:

- Yield strength of the bar should not exceed 60,000 psi (415 MPa approx.).
- Headed bar size should not increase no. 11 (36 mm approx.).
- Normal weight concrete should be used.
- Relative head area (A_{brg}/A_b) should not be less than 4.
- Clear cover shall not be less than 2 times bar diameter ($2d_b$).
- The clear spacing provided between bars shall not be less than $4d_b$.

The development length for headed bar and mechanically anchored deformed bars in tension is given as:

$$L_{dt} = \left(0.016 \frac{\Psi_e f_y}{\sqrt{f'_c}}\right) . d_b \geq \text{maximum of (8db and 152.4 mm)} \qquad \text{Eqn. 2.22}$$

where,

Ψ_e = amplification factor, taken as 1.2 for epoxy coated, otherwise 1.0

f'_c = concrete compressive strength (MPa) $\leq$ 41.4 MPa

The section 3.5.9 explains about the obstruction. It should not be more than $2d_b$ from the bearing face of the head in the deformed bar.

In the Appendix D (ACI 318, 2008), the explanation for the anchorage capacity is explained which is based on the Concrete Capacity Design (CCD) method (Fuchs et al., 1995). The CCD method is generally used for studs, expansion anchors and bolts. The surface of these are smooth and the bond capacity due to development length were not considered in the design. Hence, the results which are calculated by this method were conservative as in the case of deformed bar the bond capacity is also provided by the developed length. The failure pattern was assumed to be pyramid in which the height is equal to the embedment length and a square base is considered at the surface and the point at the head (Figure 2.17, 2.18 and 2.19).

If the headed bars were placed near the edge then the failure area decreases and the ultimate capacity decreases.

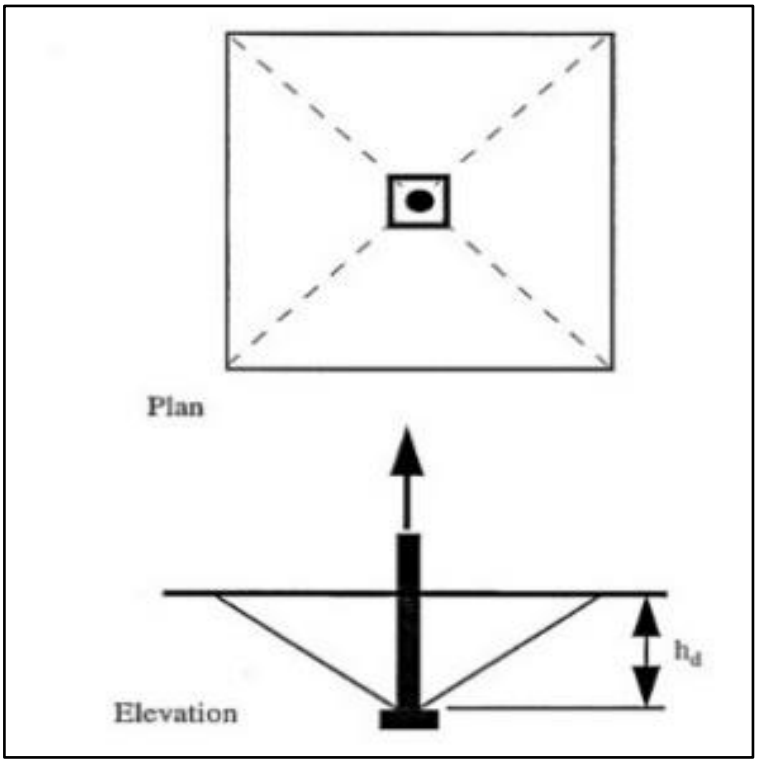

Figure 2.16: Plan and elevation of headed bar embedded in concrete (Fuchs et al., 1995)

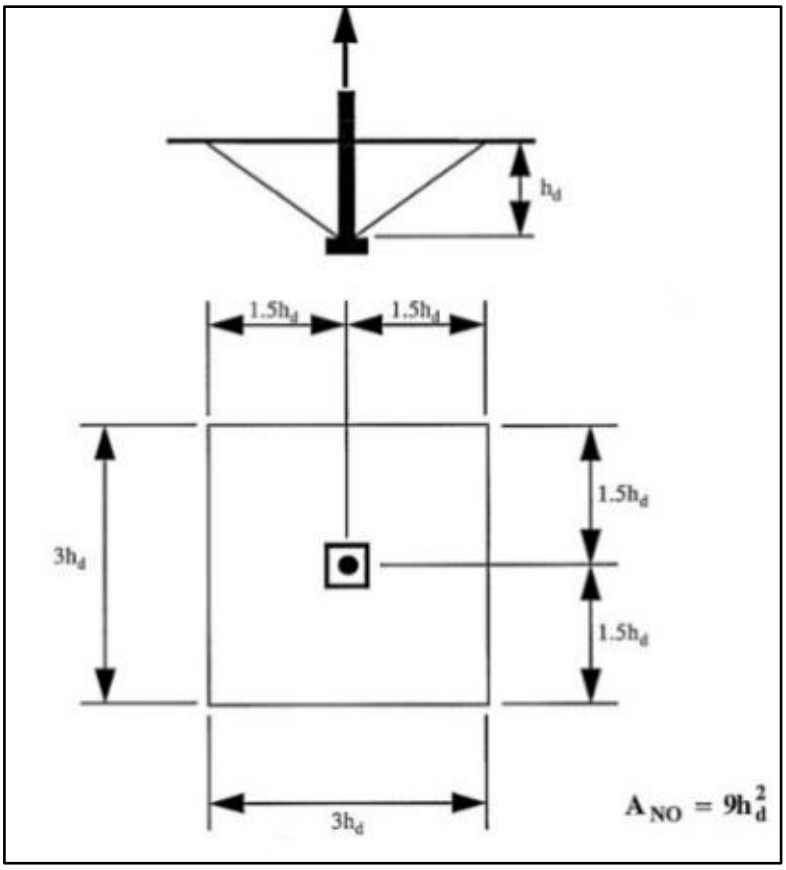

Figure 2.17: Dimension measurement of centred embedded bar (Fuchs et al., 1995)

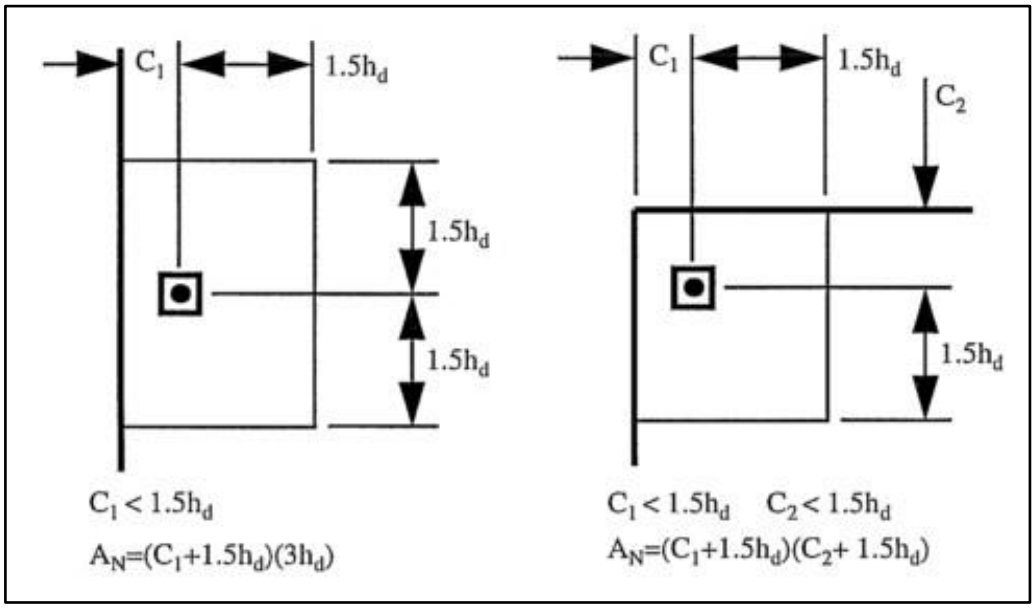

Figure 2.18: Dimension measurement of side embedded headed bar (Fuchs et al., 1995)

The pull-out capacity of single anchor bolt or headed studs when embedded at centre are calculated as:

$$P_{UO} = 0.0155\left(h_d{}^{1.5}\right)\sqrt{f'_c} \qquad \text{Eqn. 2.23}$$

When the anchor bolt is embedded near the edges then pull out capacity is calculated as:

$$P_U = \frac{A_n}{A_{No}} P_{UO} \qquad \text{Eqn. 2.24}$$

If anchor bolt or shear stud is unsymmetrical placed, the capacity is further reduced due to unsymmetrical stress distribution. To take this in account Ψ is multiplied as the reduction factor. The modified formula is given as:

$$P'_U = \Psi \frac{A_n}{A_{No}} P_{UO} \qquad \text{Eqn. 2.25}$$

$$\Psi = 0.7 + 0.3\frac{c_1}{1.5h_d} \leq 1 \qquad \text{Eqn. 2.26}$$

Where,

P_{UO} = ultimate capacity (kN)
h_d = embedment depth (mm)
P_U = modified ultimate capacity (kN)
A_n = available area (mm^2)
A_{No} = total area of square (mm^2)
f'_c = concrete compressive strength from cylinder test (N/mm^2)
Ψ = reduction factor

2.5.4.3 ACI 352R, 2002

The codal provision for headed bar to use it for beam-column joint is included in the ACI 352R, 2002. It is based on monotonic as well as cyclic loading. The development length provided by this code considers the location of headed bar and the amount of head restraining reinforcement. The development length is explained for both Type 1 and Type 2 beam-column joint connections.

The development length (in mm) for standard 90^o hooked bar for Type 1 connection is given as:

$$L_{dh} = \frac{f_y d_b}{4.2\sqrt{f'_c}}$$ Eqn. 2.27

The development length (in mm) for standard 90^0 hooked bar for Type 2 connection is given as:

$$L_{dh} = \frac{\alpha f_y d_b}{6.2\sqrt{f'_c}}$$ Eqn. 2.28

Where,

α = Stress multiplier for longitudinal reinforcement at joint/member interface for Type 2 connections

If transverse joint reinforcement is provided at a spacing less than or equal to 3db, then equation for Type 2 connection is multiplied by 0.8.

The development length for headed bar for both Type 1 and Type 2 connections are taken as $3/4^{th}$ of the development length for Type 2 hooked bar connection. In the case of headed bar, the location of headed bar should be within 50 mm from the back of confining core.

In any case, the development length calculated for the headed bar should not be less than the maximum of $8d_b$ and 150 mm. The development length calculated by the this code provision is 75% of the development length that of hooked bar whereas development length calculated by Bashandy,1996 is 60 to 65% and McCabe et al., 1997 is approximately 60%.

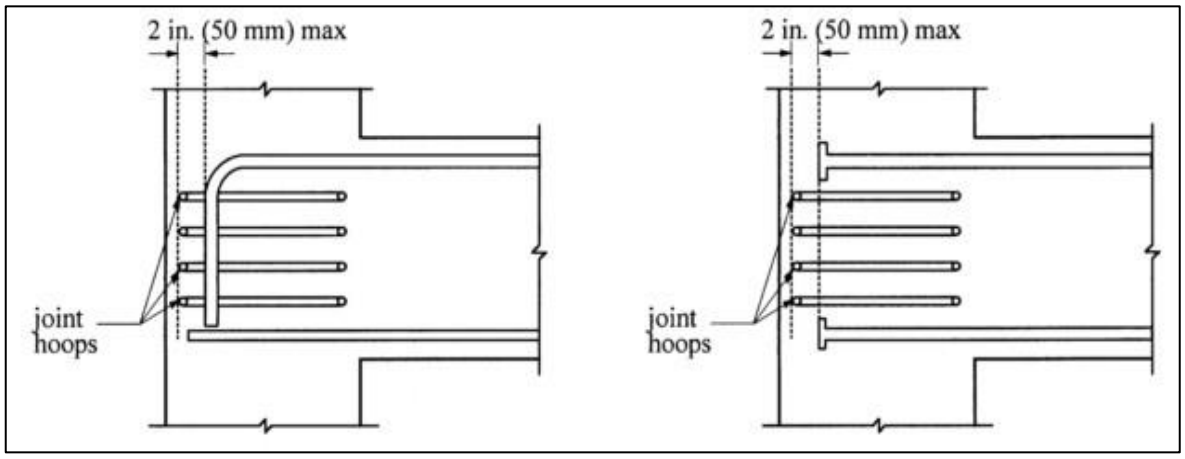

Figure 2.19: Location of headed bar (ACI 352R, 2002)

2.6 Patents registered

Very limited patents related to headed bar is registered. Some of them are explained as follows:

Kies et al., 1989 (Patent no. 4870848) invented a machine for the threading on the reinforcement bar. The main purpose of the invention was to connect the reinforcing bar with the rotating disc to use it in concrete construction work. The threaded part of the bar had tapered end and it was formed either by hot or cold forging and by cutting. The tapered thread made by the machine had uniform pitch and thread which offer an efficient reinforcing bar joint to couple the two-reinforcing bar to develop the sufficient strength to the connection.

Hiendl, 1992 (Patent no. 5131204) invented an economical and simple threaded sleeveless reinforcing steel screw connection having a conical tapered section at the one end. The connection provided high loading capacity and fatigue limits. The angle between the thread with the axis of the element made 3^0 to 10^0 and the pitch for threading were taken as 1 mm to 2.5 mm. The threaded angle was provided between 76^0 to 90^0. In the connection, the female part had a softer core and a harder cross-section for the effective transfer of tensile forces and torque.

Samas et al., 1992 (Patent no. 5158404) invented a machine for making the tapered threading in the reinforcing bar to connect it with the other bar through the coupler. The machine could be used to thread all size diameter bars by removing and replacing the control rod. Also, the speed of the cutting of thread can be control by adjusting the RPM of the machine. In this way, the threading could be done with a single machine within a short period of time.

Gruson et al., 2001 (Patent no. 6286270) invented an anchor technique for the reinforced concrete structures. The anchor was having a short axial length and have diameter one and half times to three times the diameter of the bar from which it was attached. The anchor was having the rib at the surface of the head which was provided for the extra bonding area when embedded in concrete. The rib at the head were provided in the form of continuous helix. The height of the rib was taken as one third of the pitch. For the connection of the anchor to the corresponding reinforcing bar, the threaded connection was used and the bar can be connected at one end or both end.

Lancelot III et al., 2002 (Patent no. 0189175 A1) invented an anchorage mechanism for the structural concrete. The detail of the mechanism included a metal plate which was attached at the end of the reinforcing bar by means of welding. This system can be used with improved

tensile strength and better pull-out performance in the concrete construction work. At the end of the bar which would attach with the anchor plate was forged prior to the welding. The plate shape which were attached to the bar may be of uniform diameter or it may be enlarged by forging the plate before the welding.

Bennett et al., 2006 (Patent no. 0059841) invented an anchorage mechanism which was improved compared with the other available anchor mechanism. A plate of shape either square, round, rectangular or some other configuration was attached to the reinforcing bar. An opening was provided in the plate having the diameter of the opening greater than the outer diameter of the bar. The bar was connected through the plate by preheating the bar end and then forging onto the plate. The end anchor provided by this method utilised less energy and have less cost.

2.7 Indian Scenario

In India, till now very limited work has been done regarding the attachment of mechanical device in beam-column joint. No patent has been filed on the anchorage mechanism related to beam-column joint in Indian patent database. Some of the work related to headed bar is done at NIT Surat and Mepco Schlenk Engineering College, Sivakasi, Tamilnadu. But still, its implementation at the site is not done yet due to the limited research work.

2.8 Concluding remarks

As per the literature review, the major scope of work includes understanding of guidelines of headed bars, observe the research gaps and workout a study plan. Based on the guidelines of headed bars, the research gaps observed are as follows:

- Effect of frictional grip of head on anchorage capacity
- Application of headed bar in lightweight concrete
- Application of headed bar in precast beam-column joint
- Development of an effective formula for the calculation of head dimension
- Effect of length of head on anchorage capacity
- Economical and effective headed bar

CHAPTER 3

MATERIAL CHARACTERISATION

3.1 General

The properties and behaviour of reinforced concrete are strongly influenced by the properties of its constituent materials viz. concrete and headed bar. The concrete consists of cement, fine aggregates, coarse aggregates and water in definite proportions while the headed bar consists of the reinforcement bar and the mechanical anchor i.e. head. The characteristics of concrete and reinforcement varies, depending on their mechanical properties viz. compressive strength, tensile strength, modulus of elasticity etc. The present chapter deals with the characterization of reinforced concrete and its constituent elements. A series of tests have been conducted for determining the aforementioned properties, before the pull-out testing.

3.2 Concrete and its constituents

3.2.1 Cement

Cement is the binding material in concrete. The physical and chemical properties of cement were determined as per IS 4031 (part II) and IS 4032. The cement was stored in a cool and dry place to avoid any change in its properties. The properties of cement include the standard consistency, initial setting time, final setting time and compressive strength. Cement used during the experiment is Ultra-Tech, which is OPC 43 grade (Figure 3.1). Table 3.1 shows the properties of cement.

Figure 3.1: Ordinary Portland cement 43 grade

Table 3.1: Properties of cement as per IS 4031

Parameters	Test values	As per IS 8112: 2013
Standard consistency (% of water by weight of cement)	29 %	-
Setting time (minutes)		
Initial	80	30 (min.)
Final	290	600 (max.)
Compressive strength (MPa)		
3 days	27.60	23 (min.)
7 days	36.40	33 (min.)
28 days	48.30	43 (min.)

3.2.2 Fine aggregates

The river sand has been used in the present study which falls in Zone-II category. The sand was sieved from 4.75 mm IS sieve, before using it for casting (Figure 3.2). The particle size distribution was obtained after sieve analysis as per IS 2386: 1963 (Part I). Table 3.2 shows the result of the sieve analysis.

Table 3.2: Sieve analysis of fine aggregates

IS sieve size	Weight retained (kg)	Cumulative weight retained (kg)	% Cumulative weight retained	% Cumulative weight passing
20 mm	-	-	-	-
10 mm	-	-	-	-
4.75 mm	0.080	0.080	8.9	91.1
2.36 mm	0.070	0.150	16.6	83.4

1.18 mm	0.080	0.230	25.6	74.4
600 µm	0.235	0.465	51.6	48.4
300 µm	0.332	0.797	88.5	11.5
150 µm	0.089	0.886	98.4	1.60
Pan	0.008	0.894	99.3	0.70
Total			**289.6**	
Fineness modulus = 2.90				

Figure 3.2: Sand after sieve analysis

3.2.3 Coarse aggregates

12.5 mm sieved and 20 mm sieved coarse aggregate 40 % and 60 % of the total coarse aggregate respectively were used (Figure 3.3 and 3.4). Sieve analysis is performed as per IS 2386: 1963 (Part I). Table 3.3 and 3.4 shows the result of sieve analysis for 12.5 mm down and 20 mm down aggregates respectively.

Table 3.3: Sieve analysis of 12.5 mm down coarse aggregates

IS sieve (mm)	Weight retained (kg)	Cumulative weight retained (kg)	% Cumulative weight retained	% Cumulative weight passing
20	-	-	-	-
12.5	0.143	0.143	7.51	92.48
10	0.690	0.833	43.77	56.23
4.75	0.979	1.812	95.22	4.78
2.36	0.091	1.903	100.00	0.00
0.60	-	-	100.00	0.00
0.30	-	-	100.00	0.00
0.15	-	-	100.00	0.00
Pan	-	-	-	-
Total			**546.5**	
Fineness modulus = 546.5/100 = 5.46				

Table 3.4: Sieve analysis of 20 mm down coarse aggregates

IS Sieve (mm)	Weight retained (kg)	Cumulative weight retained (kg)	% Cumulative weight retained	% Cumulative weight passing
20	0.617	0.617	30.83	69.16
16	0.911	1.527	76.31	23.69
12.5	0.447	1.973	98.60	1.40
10	0.027	2.001	100	0.00

4.75	-	-	100	0.00
2.36	-	-	100	0.00
0.60	-	-	100	0.00
0.30	-	-	100	0.00
Pan	-	-	-	-
Total			**705.74**	
Fineness Modulus = 705.74/100 = 7.05				

Figure 3.3: Coarse aggregates - 12.5 mm down

Figure 3.4: Coarse aggregates - 20 mm down

3.2.4 Water

Water is one of the most important constituent in concrete. In the present study, normal tap water was used for the casting of concrete. No admixture was added with water. Water makes the concrete workable and plays an important role in the hydration process of cement.

3.2.5 Concrete mix proportion

The concrete mix proportion per cubic meter for M20 grade is shown in the Table 3.5. For the trial mix, 150 mm concrete cubes were casted. The slump of the concrete was 125 mm. Figure 3.5 shows the slump testing and casting of concrete cube.

Table 3.5: Mix proportion for M20 grade concrete per cubic meter

Material	Quantity
Cement (kg)	360
Fine aggregates sand (kg)	750
Coarse aggregate 12.5 mm down (kg)	451
Coarse aggregate 20 mm down (kg)	677
Water (kg)	180
Water-cement ratio	0.5

(a) Slump test of concrete (b) Cube casting process

Figure 3.5: Slump testing and cube casting process

Figure 3.6 shows the concrete cube after demoulding. The testing of concrete in compression was done at UTM of capacity 1000 kN. The crack generated during compression testing and

failure pattern is shown in Figure 3.7. The average compressive strength of concrete after 7 days and 28 days were found to be 21.69 MPa and 27.66 MPa respectively.

Figure 3.6: Concrete cube specimen for compression testing

(a) Crack developed during compression testing

(b) Failure pattern observed

Figure 3.7: Concrete cube specimen during and after testing

3.3 Properties of headed bar

3.3.1 Reinforcement steel

HYSD bar was used in the present study. The yield strength was 415 MPa (Figure 3.8). The diameter of the bar was 12 mm.

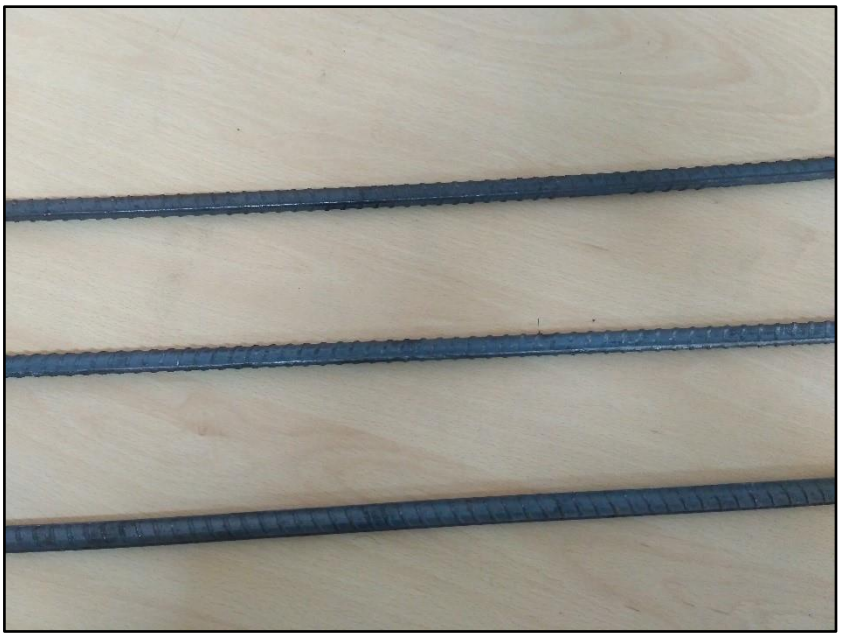

Figure 3.8: Deformed bar of diameter 12 mm

3.3.2 Mechanical anchors

Mechanical anchors was of Fe 500 grade and manufactured at the workshop. Other details are provided in section 5.2.

CHAPTER 4

NUMERICAL ANALYSIS

4.1 Introduction

For the selection of effective size and shape of the mechanical anchor, numerical analysis were done. During the failure of beam-column joint, insufficient development length and the spread of splitting crack into the joint core may results in the slippage of the bar and cause pull-out failure (Uma and Prasad, 1996). The analogy of the pull-out failure in the beam-column joint can be analysed by the tensile testing of the bar with anchor, embedded in the concrete (Figure 4.1). With the help of the tensile testing, the effective size of the anchor can be found out which can be compared with the hooked bar in beam-column joint. The tensile testing of the bar with anchor , embedded in concrete (Pull-out testing) firstly analysed numerically. The numerical analysis of the pull-out testing of the anchor is done at this chapter. Pull-out test is performed on the headed bar to estimate the pull-out capacity. In pull-out testing, different type of failure can be observed which is yield or fracture of steel, concrete side blowout failure or pull-cone failure. Yield or fracture failure occurs when the applied stress during the pull-out is greater than the yield stress of the bar and any other mode of failure does not occur before this. A pull-cone failure is defined when along with the headed bar, the surrounding concrete is also being pulled-out as a single unit (Thompson et al., 2002). Side blowout failure is defined as the spalling of the concrete cover over the head (Thompson et al., 2002). In the small ratio, the pull-cone failure is expected as the ratio increases, either side blowout failure or yielding or fracture of the bar occurs.

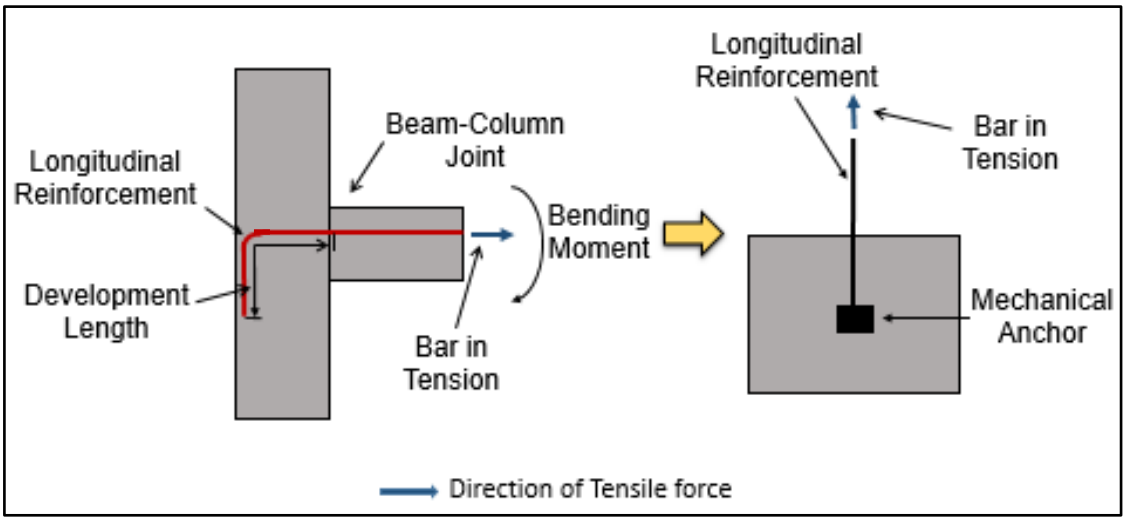

Figure 4.1: Pull out test for longitudinal bars

4.2 Finite element analysis

4.2.1 Modeling strategies

The modeling is based on Non-linear Finite Element Analysis (NEFA) as per Abaqus Standard/Explicit mode. NFEA is generally used for the analysis of complex geometry and loading which are time consuming as well as not economical. With the help of geometry of the object and its boundary condition, the expected solution can be found out. There is an extensive library of elements based on distinctive features. The characteristics of the elements used in Abaqus are as follows:

- Family
- Degrees of freedom
- Number of nodes
- Formulation
- Integration

The names of the elements are unique and based on these five features. The family include the geometry type of the element. The commonly used families in Abaqus are continuum (solid) element, shell element, beam element, rigid element, membrane element, infinite element, truss element, etc. The first letter in the element name refers to the family type. The degrees of freedom is the fundamental feature of the element. Some have translational degrees of freedom (truss elements) while some have rotational degrees of freedom (beam element). Based on the loading conditions, the degrees of freedom can be finalized. The convention followed in Abaqus for translation and rotation are as follows:

- 1 for Translation in direction 1
- 2 for Translation in direction 2
- 3 for Translation in direction 3
- 4 for Rotation about the 1-axis
- 5 for Rotation about the 2-axis
- 6 for Rotation about the 3-axis

The directions 1, 2 and 3 corresponds to the global x, y and z co-ordinate system respectively unless local co-ordinate system is defined at the nodes. The number of nodes are based on the

order of interpolation. The order of interpolation can be linear or quadratic. The displacement and rotational degrees of freedom are calculated at the nodes. The number of nodes is identified in the name of the element.

The formulation part includes the mathematical theory of the element's behaviour during analysis. There are two major types of formulation used in Abaqus – Langrangian and Eulerian. In the Langrangian formulation, the material associated with an element remains associated with the element throughout the analysis, and material cannot flow across element boundaries. In the Eulerian formulation, the elements are fixed in space as the material flows through them. It is used commonly in fluid mechanics simulations. In Abaqus software, numerical techniques integrate various quantities over the volume of the elements. It evaluates the material response at each integration point of an element. There are two types of integration in Abaqus – Full and reduced. The type of integration defines the accuracy of the result. The details of formulation and integration are shown in the name of the element. Based on the features of the elements in Abaqus, in the present study the type of element for all parts of the specimen (head, reinforcement bar and cube) is C3D4 (Continuum three dimensional four node element). The family is continuum (solid) type. The order of interpolation is linear type. The number of nodes considered is four at four corners of the element as shown in Figure 4.2. As it is pull-out test of headed bar in concrete cube, the elements of the assembled model are not going to flow beyond element boundaries. The formulation is based on Langrangian method. The integration is to be performed fully throughout the specimen. Hence full integration is adopted during analysis.

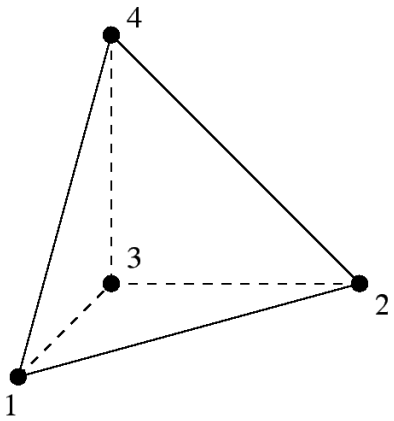

Figure 4.2: Tetrahedron element, C3D4 (Dhondt, 2014)

4.2.2 Element types

For the modeling of the pull-out testing varied materials were used. 3-Dimensional (3D) tetrahedron continuum (C) elements were selected for the analysis. These elements were also known as free elements. The reason behind selecting these elements were the irregular geometry of cube and anchor. Generally, for the 3D analysis of regular geometry, 8 noded brick elements are preferred due to its regular geometry of the elements and the number of elements after meshing creates very less. In the case of irregular geometry, these brick elements distort. It is given that with the small size of the element of the tetrahedron element, the computational cost increases but the accuracy of the result of the analysis is satisfactory (Abaqus Documentation 6.12). For the irregular geometry, these elements are preferred. Diverse types of elements used for the analysis are described in Table 4.1.

Table 4.1: Element types used

Material Type	Element Type
Concrete	C3D4
Reinforcement	C3D4
Mechanical anchor	C3D4

4.2.3 Material properties

Material properties for concrete and steel can be defined by using their standard properties like elastic properties, density, poison's ratio etc. Steel is assumed as elastic material and failure takes place linearly. Material properties for reinforcement bar, mechanical anchor and concrete are defined in Table 4.2, 4.3 and 4.4 respectively.

Table 4.2: Material properties for reinforcement bar

Properties	Values
Density	7850 kg/m^3
Young's modulus (E)	2×10^5 N/mm^2
Poisson's ratio (μ)	0.3
Yield stress	415 N/mm^2

Plastic strain corresponding to yield stress, 415 N/mm^2	0

Table 4.3: Material properties for mechanical anchor

Properties	**Values**
Density	7850 kg/m^3
Young's modulus (E)	2 x 10^5 N/mm^2
Poisson's ratio (μ)	0.3
Yield stress	500 N/mm^2
Plastic strain corresponding to yield stress, 415 N/mm^2	0

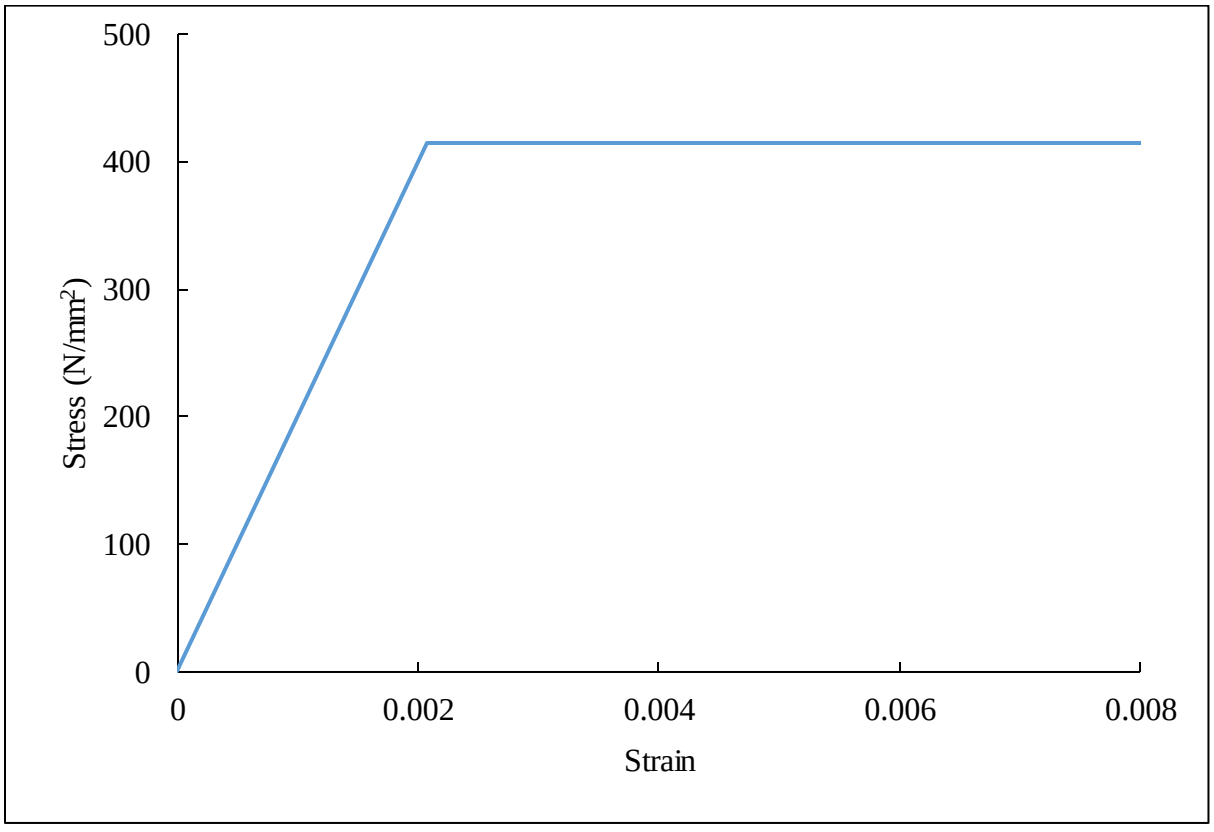

Figure 4.3: Stress-strain curve of reinforcement Fe 415 (Wu et al., 2006)

Table 4.4: Elastic properties of concrete

S. No.	Elastic Properties	Values
1	Density	2400 kg/m^3
2	Young's modulus (E)	22360 N/mm^2
3	Poisson's ratio (μ)	0.3

The stress-strain behaviour for concrete in compression is assumed as beyond the linear behaviour. The nonlinearity of concrete is a complex behaviour of concrete. The damage within the concrete was modelled as per Concrete Damage Plasticity (CDP) model which is explained later. The theoretical stress-strain behaviour for M20 grade concrete is listed in Table 4.4 (Mander et al., 1988). The behaviour of concrete in tension was modelled as tension stiffening model. The theoretical behaviour of concrete in tension was adopted as per Nayal and Rasheed, 2006. The stress-strain graph of concrete in compression and tension are shown in Figure 4.4 and 4.5 respectively.

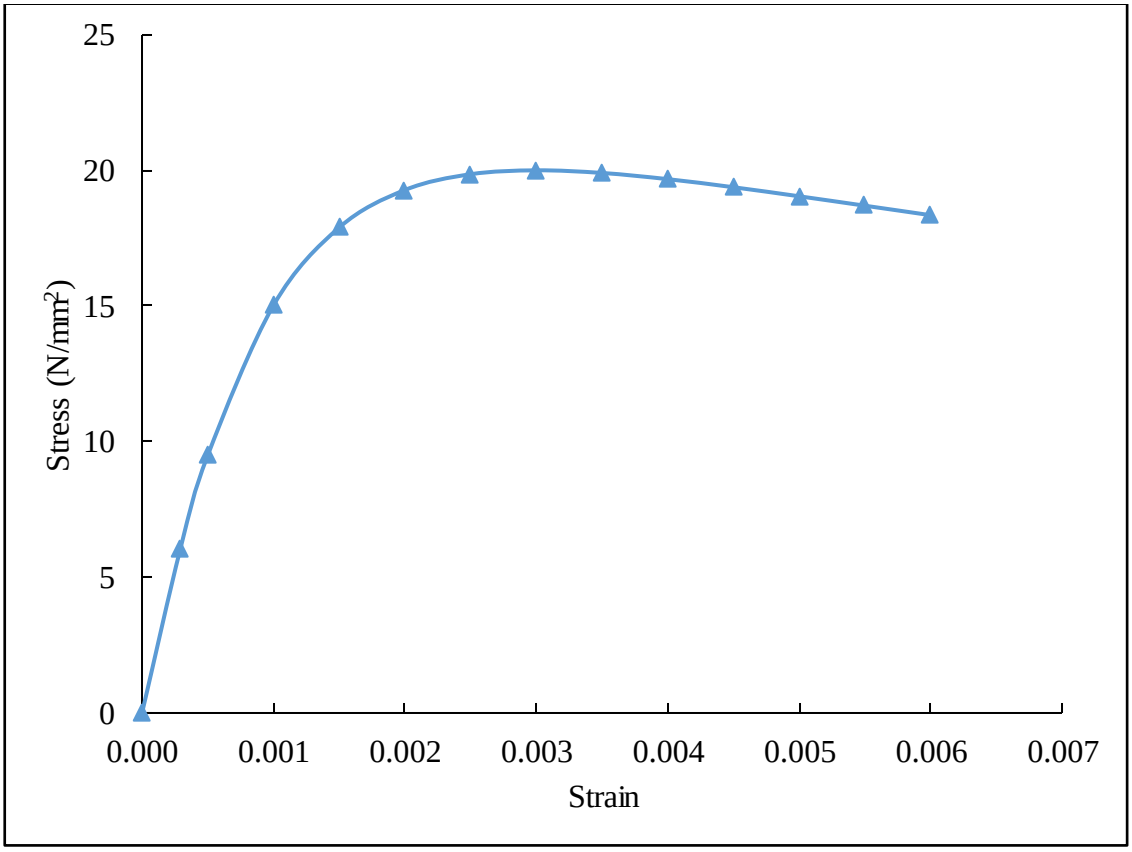

Figure 4.4: Stress-strain curve in compression (Mander et al., 1988)

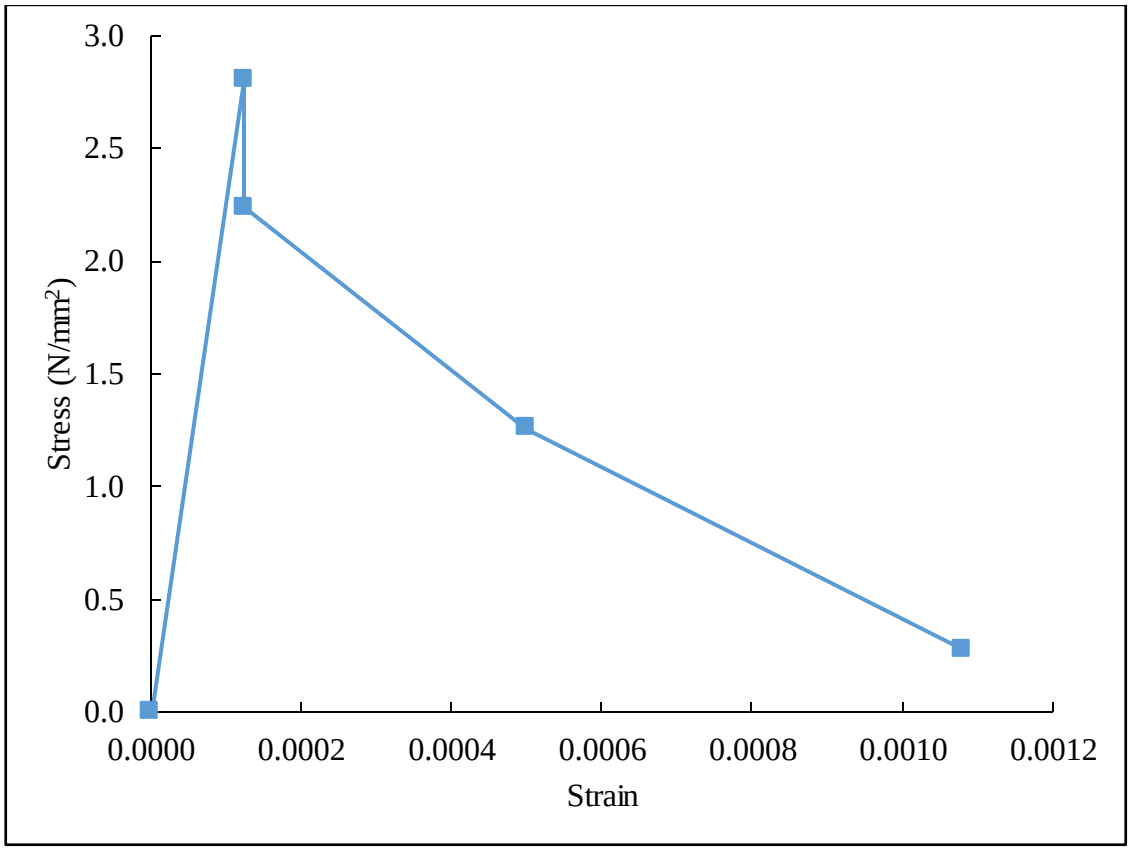

Figure 4.5:Tension stiffening model (Nayal and Rasheed, 2006)

4.2.4 Concrete damage plasticity

Beyond the linear limit of concrete, it possesses some plasticity nature. In the nonlinear behaviour of concrete, the young's modulus of elasticity of the concrete changes at every point. Damage occurs at the concrete and its behaviour in Abaqus can be modelled as smeared concrete model, brittle crack concrete model and concrete damage plasticity model (Abaqus Documentation 6.12). In the present study, concrete damage plasticity is chosen. In the plasticity damage model, the propagation of failure can be seen by the default colour notation (yellowish and reddish) in Abaqus after application of force. Damage in tension for the current model is defined by two parameters- damage parameter and cracking strain. Damage parameter in tension is defined as the ratio of cracking strain to the total strain (Abaqus Documentation 6.12).

Table 4.5: Stress-strain behaviour of concrete in compression

Stress (N/mm^2)	Strain
0.00	0.000000
6.02	0.000290
9.49	0.000500
15.02	0.001000
17.89	0.001500
19.27	0.002000
19.86	0.002500
20.00	0.003000
19.90	0.003500
19.68	0.004000
19.38	0.004500
19.04	0.005000
18.70	0.005500
18.35	0.006000

Table 4.6: Stress-strain behaviour of concrete in tension

Stress (N/mm^2)	Cracking Strain
0.00	0.000000
2.80	0.000125
2.24	0.000125
1.26	0.000500
0.28	0.001080

4.2.5 Loading

Loading in Abaqus is either applied as force or displacement loading. In the present study, displacement loading was applied for all the analysis. A maximum of 10 mm displacement loading was applied for the validation of the model and 60 mm loading was applied for analysis. At a time, maximum 10% of load was applied in the form of static and monotonic in nature.

4.2.6 Model convergence

The convergence of the model depends on two check - force equilibrium check and displacement correction check. In the force equilibrium check, the condition given in Equation 4.1 should satisfy.

$$R_a = P - I_a \qquad \text{Eqn. 4.1}$$

For the linear solution, the value of R_a becomes zero when the equilibrium is achieved. In the case of non-linear solution even after achieving equilibrium R_a never becomes zero. Due to this reason, a tolerance value is provided to achieve the solution. The default value in Abaqus is taken as 0.5% of average force in the structure. If the solution is not achieved then further iteration is required.

For displacement correction (C_a) check, the displacement correction (Equation 4.2) should be less than 1% of the incremental displacement. Same as force equilibrium, if the criteria are not achieved in this case then again further iteration is required.

$$\Delta U_a = U_a - U_o \qquad \text{Eqn. 4.2}$$

If both the criteria are satisfied then the solution is said to be converged (Abaqus Documentation 6.12).

4.2.7 Interaction

Interaction between concrete and reinforcement was surface to surface interaction (standard). For the interaction, properties were defined in normal and tangential direction. The interaction was assumed as friction interaction between steel and concrete. The frictional coefficient was taken as 0.57 (Rabbat et al., 1985). For the mechanical anchor and concrete, same interaction was provided. It is assumed that the connection between reinforcement and mechanical anchor will not fail in any case (ASTM A970/ A970M, 2016).

4.2.8 Meshing or discretization

As the geometry of the anchor and concrete cube are irregular, free meshing was used for cube, reinforcement and mechanical anchor. The approximate global size of meshing for model used in the validation is taken 8 mm. For final analysis, a mesh size of 5 mm was taken. In both the cases, meshing was done in the whole assembly at the same time.

4.2.9 Boundary conditions

Boundary condition is an important parameter during analysis. For the present study, the boundary condition was provided as fixed at the bottom of the cube so that its upward movement was restricted during the application of uniaxial pull-out force.

4.2.10 Failure type

The possible pull-out failure for headed bars are side-split failure, pull-cone failure and bar or ductile failure. Yield or fracture failure occurs when the applied stress during the pull-out stress is greater than the yield stress of the bar. Any other mode of failure does not occur before this type of failure. A pull-cone failure is defined as when along with the headed bar, the surrounding concrete is also being pulled-out as a single unit (Thompson et al., 2002). Side blowout failure is defined as the spalling of the concrete cover over the head (Thompson et al., 2002). These types of failure patterns are mainly governed by the ratio of embedment depth to side concrete cover. In the small ratio of embedment depth to side concrete cover, the pull-cone failure is expected as the ratio increases, either side blowout failure or yielding or fracture of the bar occurs. Other factors which govern the failure pattern are grade of concrete, diameter of the bar, bearing area of head etc.

4.2.11 Validation of model

The present model was validated with the theoretical value of pull-out capacity as per IS 456, 2000. For the validation of model, 100 mm cube was modelled as per IS 2770-1, 1967 with 12 mm diameter reinforcement. Two parts were modelled for the analysis - concrete cube and reinforcement. The embedment length of the bar was taken as 50 mm. The load is applied at the free end of the bar. Tensile loading was applied in which bar was pulled in the upward direction by providing fixity at the bottom part of the cube. No confinement was provided within the concrete cube. The assemblage of the model is shown in Figure 4.6. The interactions were provided at interfaces as per section 4.2.7. The mesh size was taken as 8 mm for validation and other details regarding meshing or discretization were provided in section 4.2.8. The boundary conditions for the model was same as given in section 4.2.9.

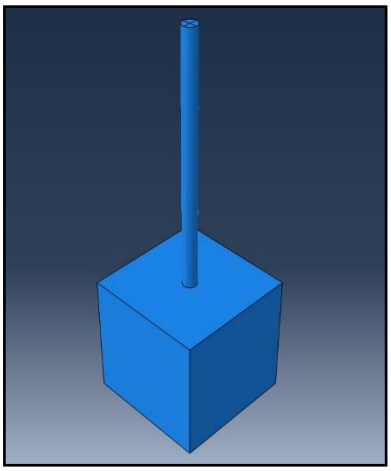

Figure 4.6: Validation of model when subjected to monotonic loading

The maximum pull-out capacity was observed as 4 kN. The load vs displacement graph is shown in Figure 4.7.

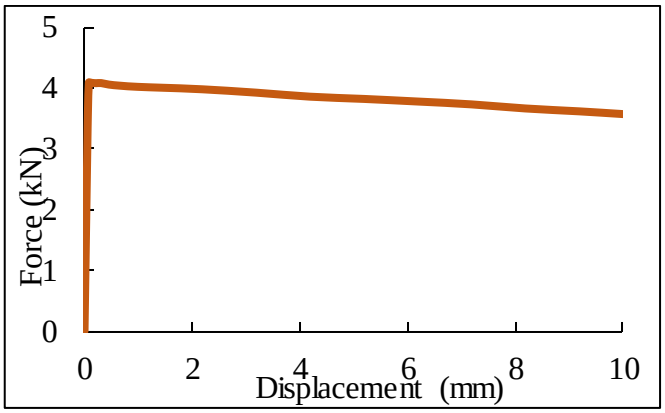

Figure 4.7:Force vs Displacement for pull-out of reinforcement

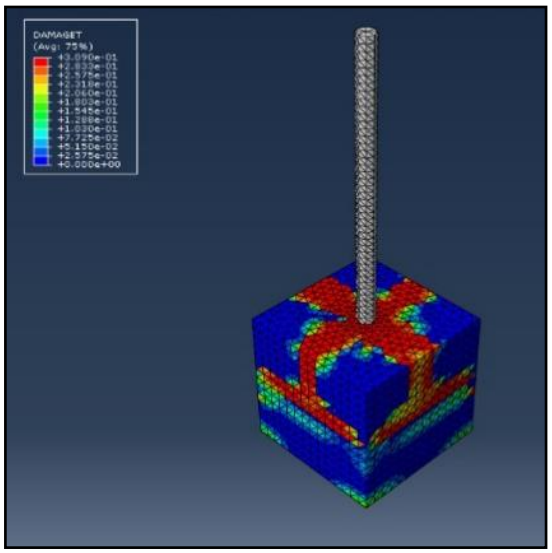

Figure 4.8: Side split failure for lesser concrete cover (Red marks shows the failure zone in the Abaqus Model)

As per IS 456, 2000 formula for pull-out capacity of the bar can be calculated as per Equation 4.3.

$$T = (\pi d_b \times L_d) \times \tau_{bd} \qquad \text{Eqn. 4.3}$$

Theoretical value of the pull-out force with 12 mm diameter bar, 50 mm development length can be calculated as,

$D_b = 12$ mm, $L_d = 50$ mm

τ_{bd} = 1.2 X 1.6 = 1.92 N/mm^2 (Section 26.2.1, IS 456, 2000)

Hence, the Pull-out Capacity = 3.72 kN

The variation in the theoretical result and numerical result are 12.7% which is reasonably acceptable (as per Abaqus Documentation 6.12).

4.2.12 Modeling of test specimens

For the analysis of pull-out behaviour of headed bar embedded in concrete, three parts were modelled separately - concrete cube, reinforcement bar and mechanical anchor. Concrete cube of size 300 mm was used for all analysis in M20 grade concrete. Mechanical anchors which were used during the analysis is of three types - plain, grooved and ribbed. The gross diameter of the anchor is taken as 27 mm for 12 mm diameter reinforcement. For the application of mechanical anchor, a minimum relative area of 4 times the cross-section area of the bar is recommended (ACI 318, 2014). In the present study, the minimum recommended relative area was obtained as 444%. The properties of mechanical anchors are listed in Table 4.7.

As per literature review, no significant work had been done on the effect of length and deformation of heads. Assuming the gross diameter of head as reference, the length of head was modelled equal to gross diameter of head i.e. 27 mm. To understand the effect of length, four more lengths were assumed. Two lengths more than 27 mm i.e. 35 mm and 43 mm; and two lengths less than 27 mm i.e. 19 mm and 11 mm were taken. The pull-out capacity could be increased by increasing the bearing area of head (Kang et al., 2010). Due to restrictions of clear bar spacing as per ACI 318, 2014, the head size is difficult to increase. Similarly, there is a provision of minimum size of head (ACI 318, 2014). Hence, to increase the pull-out capacity, there is a need to increase the bearing area of the mechanical anchor. The bearing area can be increased by increasing the number of deformations (i.e. grooves or ribs) transverse to the direction of the length of head. So, initial deformations were assumed as semi-circular with 4

mm diameter spaced at a centre to centre distance of 8 mm (Figure 4.13 and Figure 4.14). Based on the dimension of the length of heads, as the length increased, more number of deformations were provided. Thus, the type of heads were Plain heads, Grooved heads and Ribbed heads. The grade of steel used were Fe 500. The grade and diameter of reinforcement bar were Fe 415 and 12 mm respectively. The head and the reinforcement bar were threaded and attached together. The Plain head has no patterns on the outer cylindrical surface. The Grooved head has uniform semi-circular grooves of 4 mm diameter placed symmetrically around the outer surface perpendicular to the longitudinal axis of head. Similarly, the Ribbed head has uniform semi-circular ribs of 4 mm diameter placed symmetrically around the outer surface perpendicular to the longitudinal axis of head. So, the number of grooves (for Grooved head) or ribs (for Ribbed head) for 11 mm, 19 mm, 27 mm, 35 mm and 43 mm length of anchors are 1, 2, 3, 4 and 5 respectively. A total of 15 types of analysis were done. When the head is attached with the reinforcement bar then it is known as headed bar. The assemblage of the headed bar is shown in Figure 4.14.

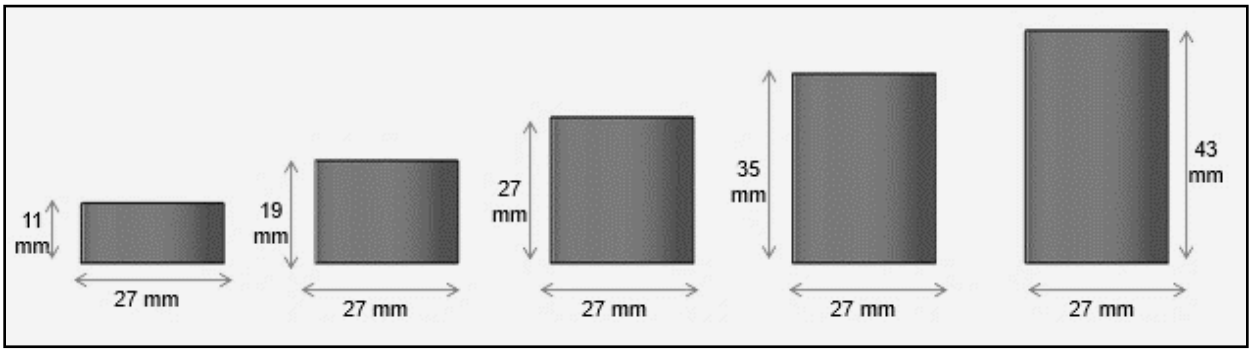

Figure 4.9: Plain head sample models

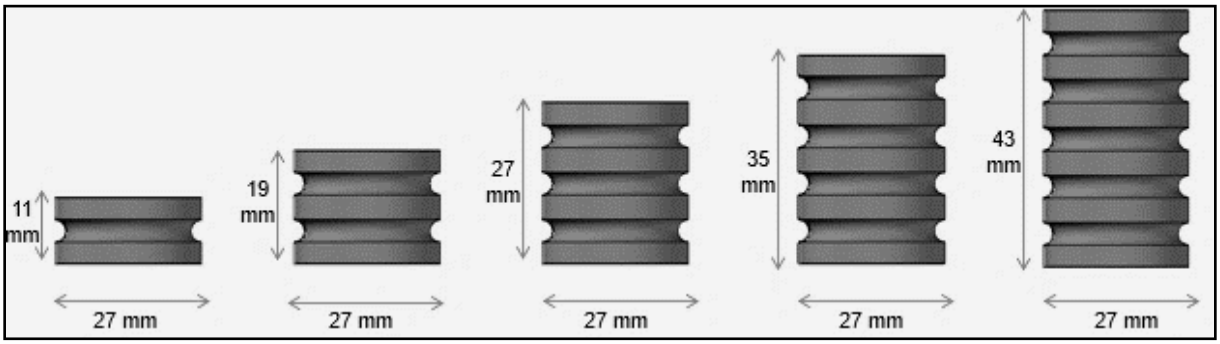

Figure 4.10: Grooved head sample models

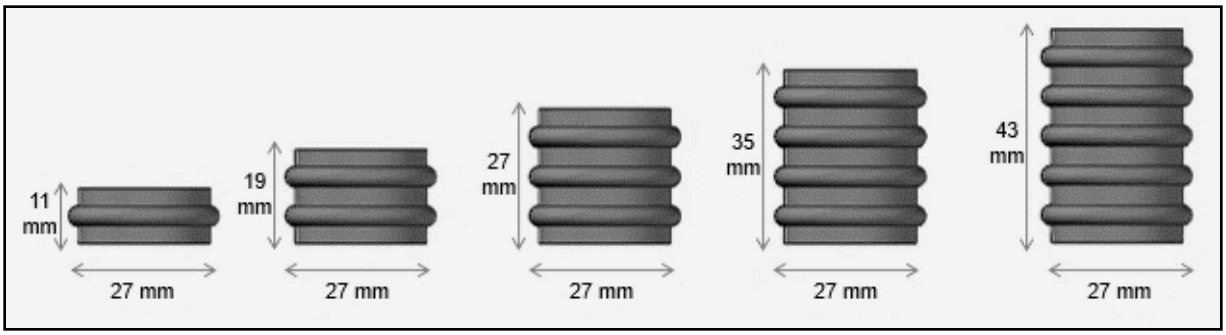

Figure 4.11: Ribbed head sample models

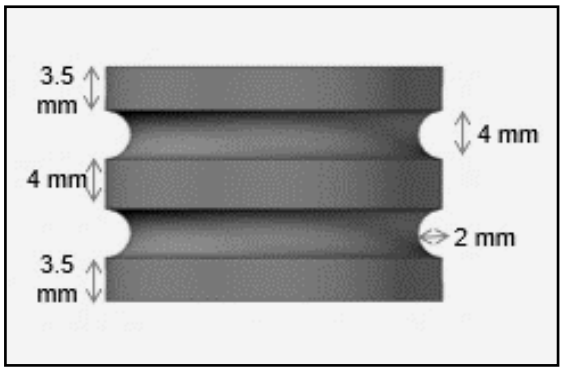

Figure 4.12: Grooved Head dimensions (Specimen - G2L19)

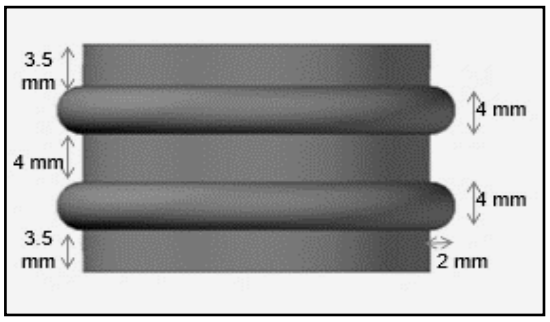

Figure 4.13: Ribbed Head dimensions (Specimen - R2L19)

Figure 4.14: Headed bar

The embedment depth for all the analysis was taken as 134 mm (Kang et al. 2010). This embedment depth was taken for getting either pull-cone failure or ductile failure. Pull-out load was applied at the free end of the bar which was applied by fixing of the concrete cube at the bottom part.

4.2.13Notation of the anchor

The notation of the different analysis was as per the usage of mechanical anchors. The plain, grooved and ribbed anchor were denoted by P, G and R respectively. The number of grooves or ribs made over the length of head were denoted by numerical digits - 1, 2, 3, 4 and 5 along with the different type of anchor notations. The length of the anchor was denoted by L and numerical digit which denotes the value of length in mm. Samples examples are shown in Figure 4.12 and 4.13. Example of this notation is, groove anchor with 3 grooves and 27 mm length is denoted by G3L27. Detail of all the different anchor used are shown in Table 4.7 with the notation.

Table 4.7: Details of mechanical anchors and their sample notations

Parameters		**Notations**				
Length (mm)		11	19	27	35	43
Number of grooves or ribs (no deformations in plain samples)		1	2	3	4	5
Anchor type	Plain	PL11	PL19	PL27	PL35	PL43
	Grooved	G1L11	G2L19	G3L27	G4L35	G5L43
	Ribbed	R1L11	R2L19	R3L27	R4L35	R5L43

No confinement was provided in the concrete. The free end of the bar for the analysis was taken as zero for getting proper damage pattern and failure of the bar. The assemblage of the pull-out specimen for headed bar and after discretization is shown in Figure 4.15.

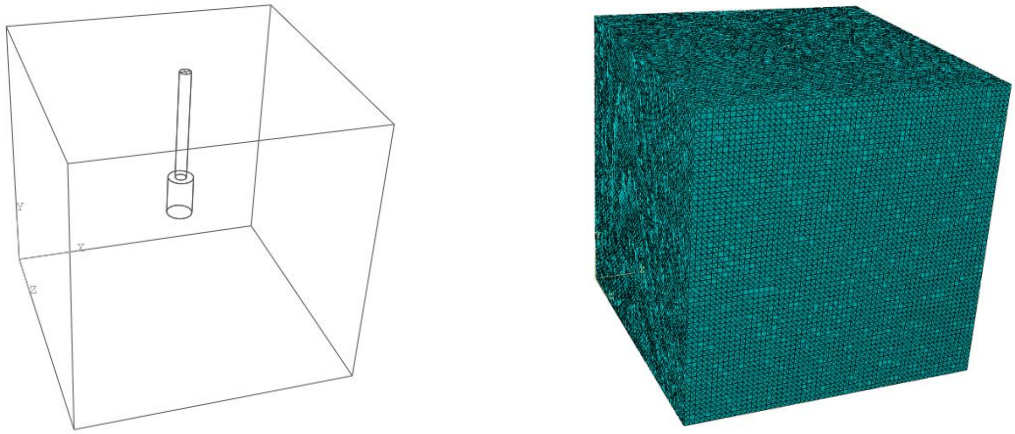

a) Cube with headed bar, transparent view b) Discretization model

Figure 4.15: Cube with headed bar

4.3 Limitations

- The major limitations of the project are the absence of deformation of HYSD bar (Fe415). Although there is absence of deformation on the bar, it won't affect much as the values of ultimate force for headed bars are higher than conventional hooked bars.
- The numerical modeling is done to check the ultimate force for headed bars. The ribbed headed bars are not modelled in Abaqus for validation with the experimental model as the ultimate force of plain headed bars are higher than the ultimate force of conventional hooked bars.

4.4 Summary

The numerical studies of the pull-out behaviour of the mechanical anchor was done to check the effective size of the anchor. Abaqus software is used for the analysis which is based on the Nonlinear Finite Element Analysis. 15 different types of anchor attached at the bar end was used during the analysis which was embedded in the 300 mm size concrete cube. The results of the analysis is shown in result and discussion chapter.

CHAPTER 5

EXPERIMENTAL INVESTIGATIONS

5.1 Introduction

Pull-out test is performed on the headed bar to estimate the pull-out capacity. The different failure pattern during testing is already explained in section 4.1. The experimental investigation was based on the pull-out behaviour of headed bar embedded in concrete cube. The dimension of the cube is decided based on the Concrete Capacity Design method (Fuchs et al., 1995). The dimension of the head is decided as per ACI 318, 2014. For the experiment, M20 grade concrete and 12 mm diameter bar is used. The bond between the concrete, the reinforcement bar and the head provides the required strength for anchorage. The major steps of experiment are fabrication of mechanical anchor, casting of concrete cubes of size 300 mm, assembling head and reinforcement bars with strain gauges and testing of final specimen.

5.2 Development of headed bar

5.2.1 Fabrication and assembling

As the explanation described in the numerical analysis, the same dimension were fabricated for the experimental investigations. The mechanical anchors were fabricated from a long cylindrical solid rod in the workshop. Firstly, the rod was fixed at the revolving lath machine. The diameter of the anchor was maintained through the trimming of the surface. With the help of Vernier calliper, it was measured accurately. After the diameter measurement, threading was made at the anchor. After threading, grooves or ribs were made. Then, it was cut from the long cylinder and finishing of threading was done manually at the lathe machine. The manufacturing process of mechanical anchor is shown in Figure 5.1. The different types of anchors plain, grooved and ribbed are shown in Figure 5.2, 5.3 and 5.4 respectively. A comparison of types of deformations are made in Figure 5.5.

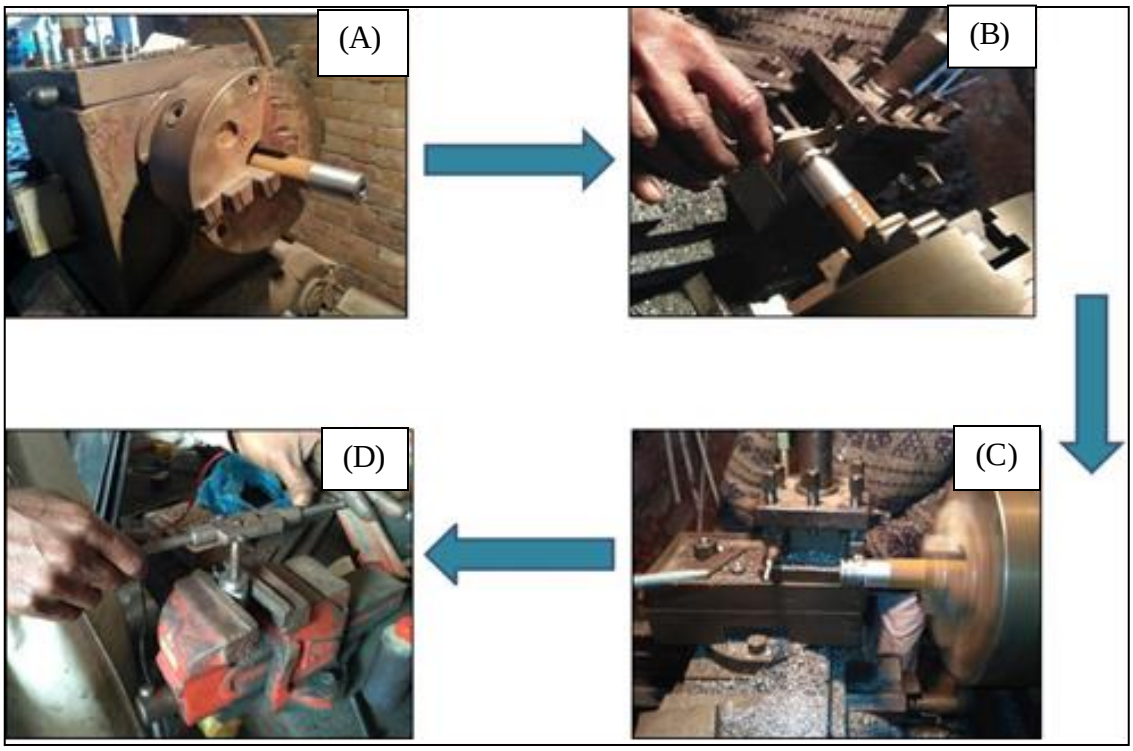

Figure 5.1: (A) Fixing of cylindrical rod (B) Measurement by Vernier calliper (C) Threading and making deformations (D) Finishing of threading

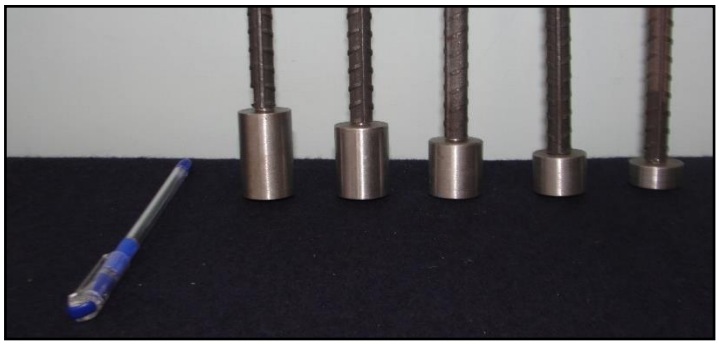

Figure 5.2: View of plain mechanical anchor fixed to rebar

Figure 5.3: View of Groove mechanical anchor fixed to rebar

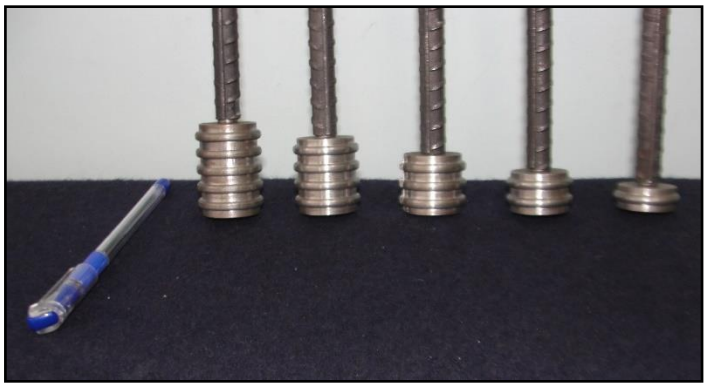

Figure 5.4: View of Ribbed mechanical anchor fixed to rebar

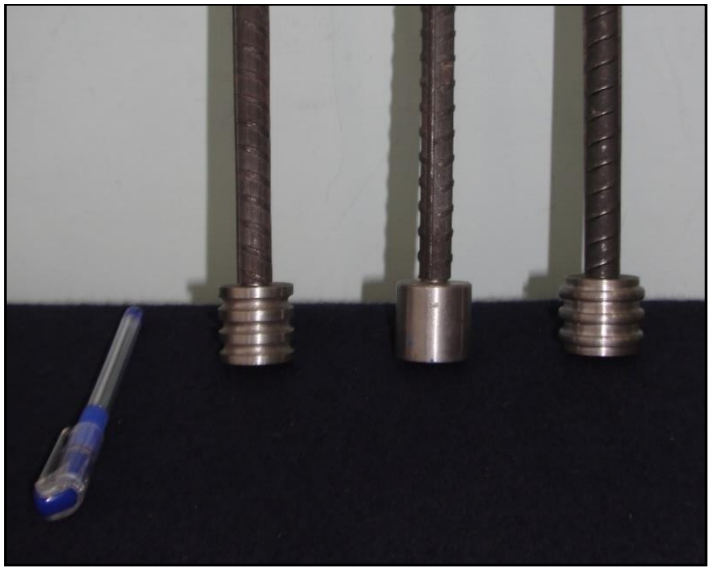

Figure 5.5: Comparison of different mechanical anchors

5.2.2 Concrete cube specimen

The dimension of the cube for pull out test is based on the pull-cone failure. The failure of concrete occurs in the conical shape with a maximum angle of 45^0 with the horizontal axis (Fuchs et al., 1995). Considering the maximum angle of cone, the effective diameter of failure cone will be,

$h_{ef} + d_h + h_{ef} = 134 + 27 + 134 = 295$ mm (Figure 5.6)

Based on the failure, the size of the cube is taken as 300 mm.

The notation of the test specimen is as per the mechanical anchor used during casting which is explained in section 4.2.13.

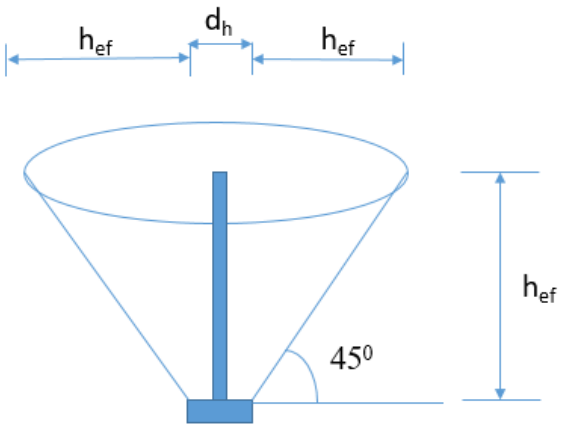

Figure 5.6 Cone failure (Fuchs et al., 1995)

Three sets of specimen are casted for each mechanical anchor and three samples are casted with only deformed bar without mechanical anchor with the same embedment depth. For each specimen, a 100 mm cube are casted for checking the compressive strength of the concrete during the testing. Hence, total 48 specimen of size 300 mm are casted for pull-out testing and 48 specimen of 100 mm are casted for finding compressive strength. One set of specimen with plain, groove, ribbed and without head are shown in Figure 5.7, 5.8, 5.9 and 5.10 respectively.

a) PL11-MS b) PL19-MS c) PL27-MS

d) PL35-MS e) PL43-MS

Figure 5.7: Different type of plain headed main specimen (MS)

a) G1L11-MS

b) G2L19-MS

c) G3L27-MS

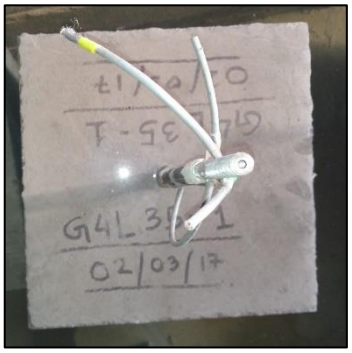

d) G4L35-MS

e) G5L43-MS

Figure 5.8: Different type of grooved headed MS

a) R1L11-MS

b) R2L19-MS

c) R3L27-MS

d) R4L35-MS

e) R5L43-MS

Figure 5.9: Different types of ribbed headed MS

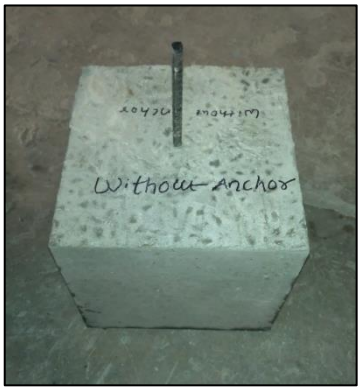

Figure 5.10: Cube specimen without mechanical anchor

5.3 Curing of specimen

Curing of concrete is very necessary at the early stage of hardening to obtain its appropriate strength. It helps in the hydration process of cement and maintain the control temperature within the concrete (Neville, 1995). 28 days curing were done for the casted specimen. Curing of the specimen are shown in Figure 5.11.

Figure 5.11: Curing of the specimen

5.4 Test setup

The experimental setup consists of the Digital Universal Testing Machine and the instrumentation. The test was conducted at the Universal Testing Machine of maximum capacity 1000 kN. A special arrangement was made to perform the test. Two plates of dimension of 750 mm x 580 mm x 25 mm was fixed on top and bottom of the Lower crosshead

with 4 bolts of 32 mm diameter. The specimen was placed on top of the upper plate. In the upper plate four oval shaped holes were made at centre to centre of distance 360 mm across the specimen and 250 mm along one side of the specimen as shown in Figure 5.12. The dimension of the oval shaped holes was 100 mm x 18 mm. The specimen was placed centrally on the upper plate. Two U-shaped steel strips of width 50 mm and thickness 12 mm at the horizontal portion and 6 mm at the vertical portion was used to fix the specimen with the upper plate. It was fixed with eight bolts of 16 mm diameter. Stiffeners were provided throughout the length on the vertical portion of the steel strip to prevent it from bending. V-shaped cuts (at an angle of 45 degrees with horizontal) were provided at the lower part of vertical portion of steel strip for providing space for tightening of the bolts. At the lower junction of horizontal and vertical portion of steel strip, triangular shaped stiffeners were provided. Two 12 mm diameter cut pieces were welded at the bottom part of the upper plate around each hole so that the head of the bolt do not rotate during tightening of the nut. The position of the cube specimen could be centred either by adjusting bolts in oval shaped holes or the plates. The free end of the embedded reinforcement bar was fixed to the Upper crosshead. A overall view of test setup is shown in Figure 5.15. Fixing of plate and cube are shown in Figure 5.13 and holes made in the upper plate for adjusting the cube are shown in Figure 5.14.

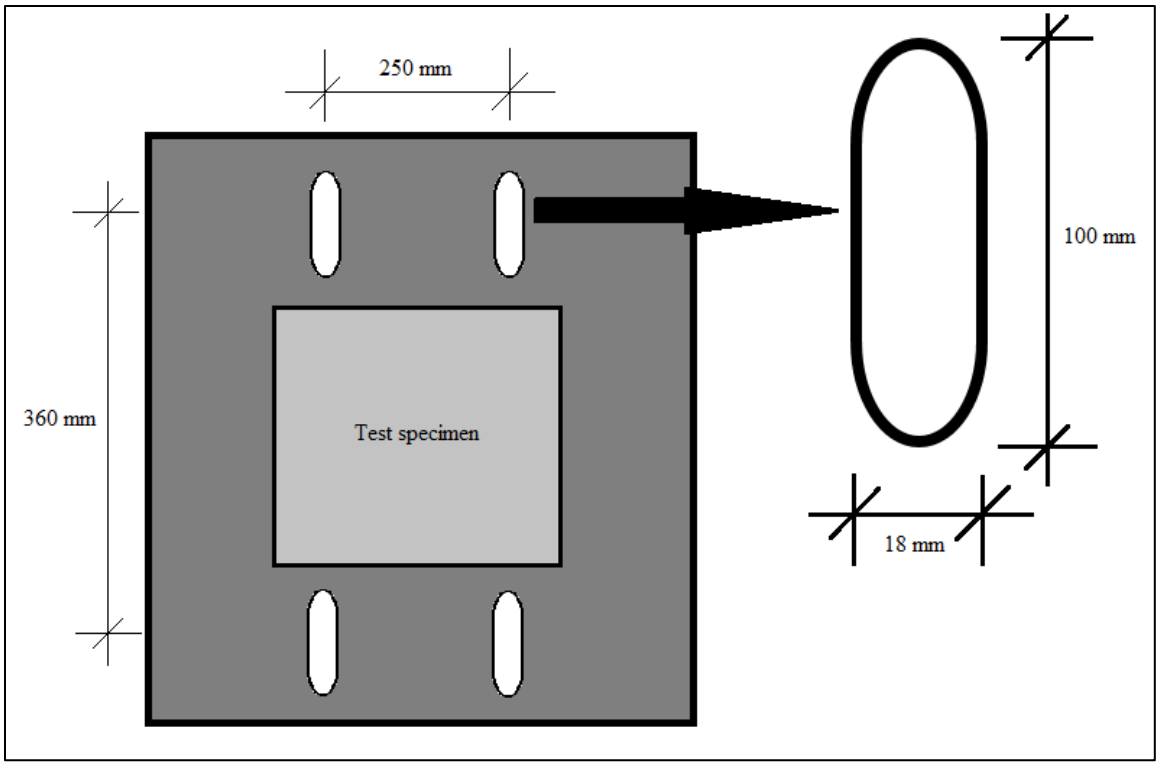

Figure 5.12: Dimensions of upper plate and its oval shaped holes

Figure 5.13: Test setup with display unit

Figure 5.14: Test setup showing upper and lower plates fixed by bolting with UTM

5.5 Instrumentation and measurement

5.5.1 Installation of strain gauges

The strain gauges were installed to monitor the strains on the headed bars during the execution of tests. The type of strain gauge used for steel is of 5 mm length with gauge factor 2.13. There are two strain gauges that are attached to the headed bar, first one is on the head which is denoted as SG1 and the second one is on the reinforcement bar near the top surface of the concrete denoted as SG2. Proper plain surface are made before the installation the strain gauges. Strain gauge SG1 and SG2 are shown in Figure 5.15 and 5.16 respectively. Water proofing of gauges were done using araldite epoxy resin adhesive and doctor's tape (Figure 5.17).

Figure 5.15: Strain gauge at the surface of reinforcement bar near the top concrete surface end (SG1)

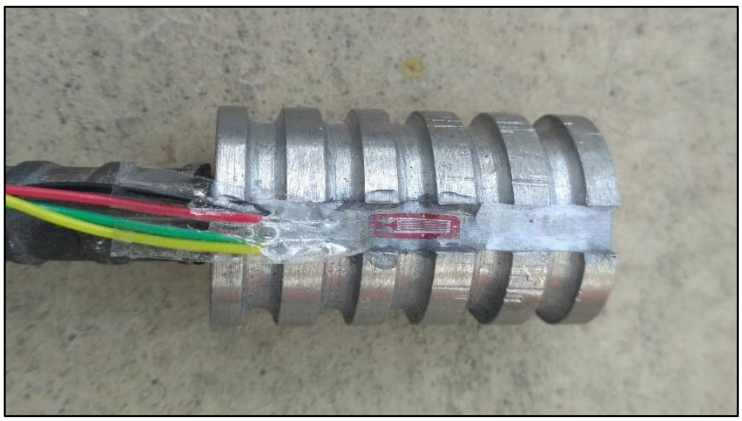

Figure 5.16: Strain gauge on the head surface (SG2)

The headed bar for different types of mechanical anchor are shown in Figure 5.17.

Figure 5.17: Different type of headed bar used during experiment

5.5.2 Measurement of strain

Strains were recorded by the 60 channel data acquisition system. Computer is connected with the data acquisition system for recording the data. The strain were recorded through the software "System 5000". The whole system is shown in Figure 5.18.

Figure 5.18: System with data acquisition for strain recording

5.5.3 Measurement of force and displacement

The force corresponding to the displacement were recorded in the system connected with the UTM. During the testing force vs displacement curve can be seen. The system connected with UTM is shown in Figure 5.19.

Figure 5.19: System connected with UTM

5.6 Test procedure

The casted specimen after curing was removed from the water tank. The specimen was put outside for air drying. Now upper and lower plate were fixed with 32 mm diameter bolt at UTM. From the upper plate, 8 bolts of diameter 16 mm were inserted making the thread in the outside direction. The specimen was put at the upper plate. The U-type steel strips were put from the upper portion of the cube. The specimen were fixed with the bolt. The proper fixing and tightening were shown in Figure 5.20.

Figure 5.20: Fixing the specimen

Connections were made for the recording of the strain. The free end of the bar is gripped properly for the force transfer. Metal plate liner were used with the grip for adjusting the hole between the grip for 12 mm diameter bar. In the computer connected with the UTM, TRAPEZIUM2 material testing software were used. Preliminary data like type of testing, maximum force, batch number, cross-sectional area of reinforcement, grip length, rate of loading etc. were feed. The details of the data provided are shown in Table 5.1. Photos were taken during the testing for visualising the failure mode and for the report preparation.

Table 5.1 Preliminary data used before testing

Type of testing	**Tensile**
Cross-sectional area of bar (mm^2)	113
Grip length (mm)	30
Rate of loading (mm/min.)	1
Sampling rate (per second)	10

CHAPTER 6

RESULTS AND DISCUSSION

6.1 General

The results of the numerical and experimental investigations on the pull-out behaviour of reinforcement bar, with and without anchor (embedded in concrete) are presented in this chapter. A comparison has been made between the pull-out capacity of the reinforcement bar with and without anchor. Finally, the results of numerical investigation are compared with the experimental results.

6.2 Numerical results

After the analysis of the model, different types of results were generated. Maximum load, deflection, cracking or damage pattern can be seen from the analysis result. Different parametric studies were done.

6.2.1 Effect of length of mechanical anchor on pull-out capacity

With the different length of the mechanical anchors, the pull-out capacity of the headed bars was analysed. The load vs displacement curve for the 5-different length of anchors were analysed. For plain bar, the maximum pull-out capacity was found for 19 mm length of mechanical anchor which is 47.52 kN corresponding to a total of 60 mm displacement loading. Similarly, for grooved headed bar, again the maximum pull-out capacity was found for 19 mm length of mechanical anchor corresponding to a total of 60 mm displacement loading which was 47.05 kN. For the ribbed headed bar, the maximum pull-out capacity was found for 11 mm length of mechanical anchor for a total of 60 mm displacement loading which was 46.68 kN. The load vs displacement curve with different lengths of mechanical anchor for plain, grooved and ribbed headed bar is shown in Figure 6.1, 6.2 and 6.3 respectively. The notation for specimens were discussed in Chapter 4.

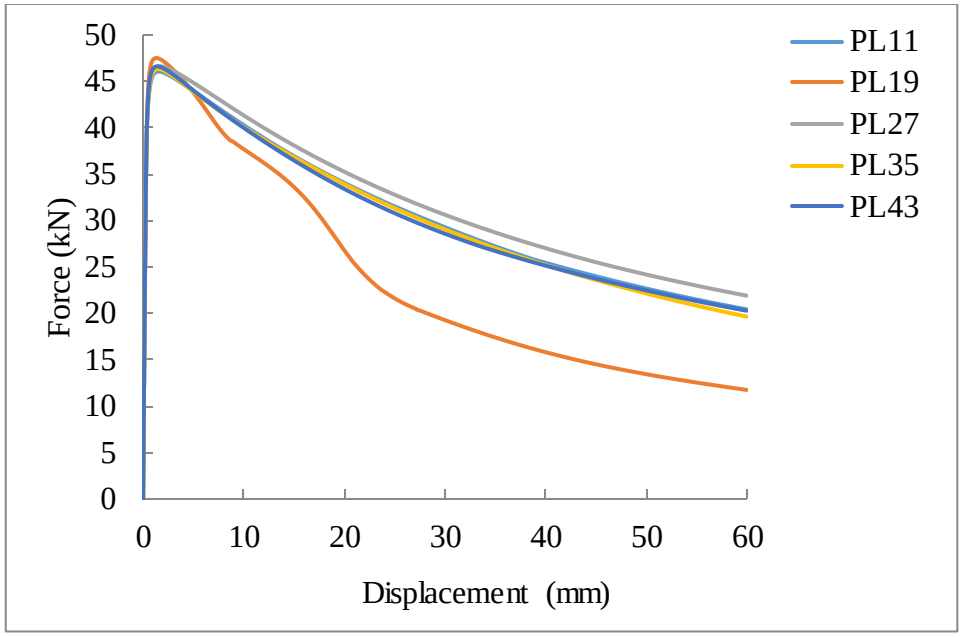

Figure 6.1: Pull-out capacity of headed bar for different length of mechanical anchor for plain headed bar

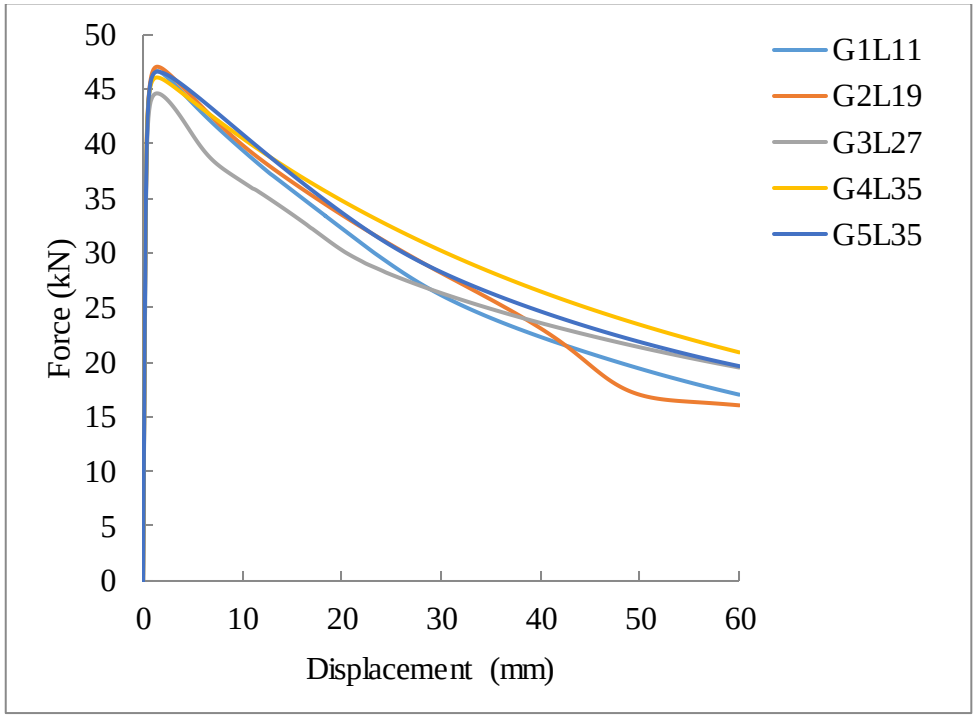

Figure 6.2: Pull-out capacity of headed bar for different length of mechanical anchor for grooved headed bar

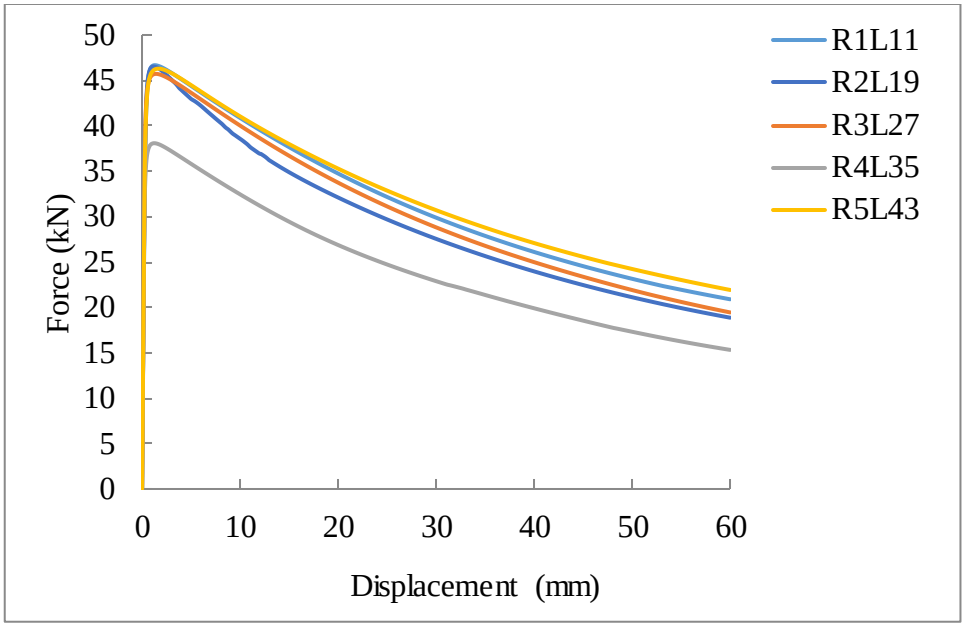

Figure 6.3: Pull-out capacity of headed bar for different length of mechanical anchor for ribbed headed bar

6.2.2 Effect of deformation over the length of mechanical anchor on pull-out capacity

The load vs displacement graphs were plotted with the same length of the mechanical anchor but with distinct types of deformations over the length. These deformations were plain, grooved and ribbed. The load vs deformation curve for 11 mm, 19 mm, 27 mm 35 mm and 43 mm length of mechanical anchor with different deformations are shown in Figure 6.4, 6.5, 6.6, 6.7 and 6.8 respectively.

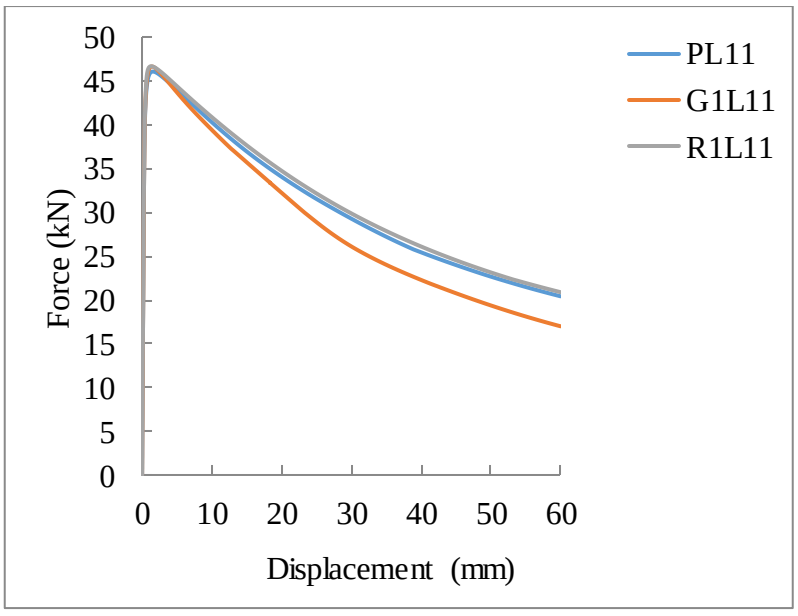

Figure 6.4: Effect of deformation over length for 11 mm length of mechanical anchor

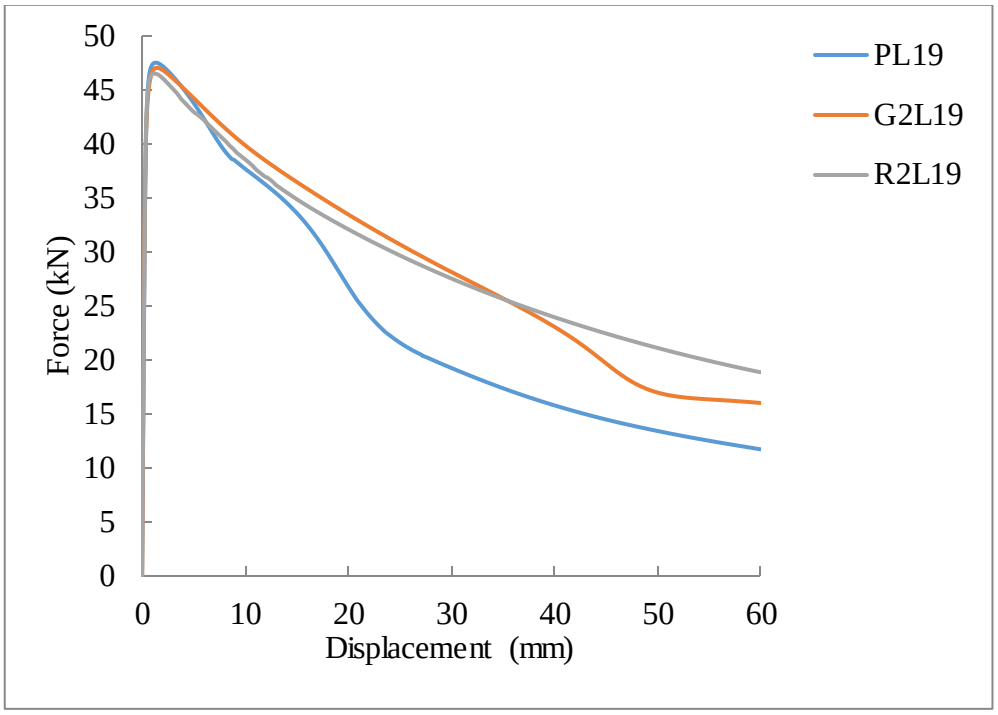

Figure 6.5: Effect of deformation over length for 19 mm length of mechanical anchor

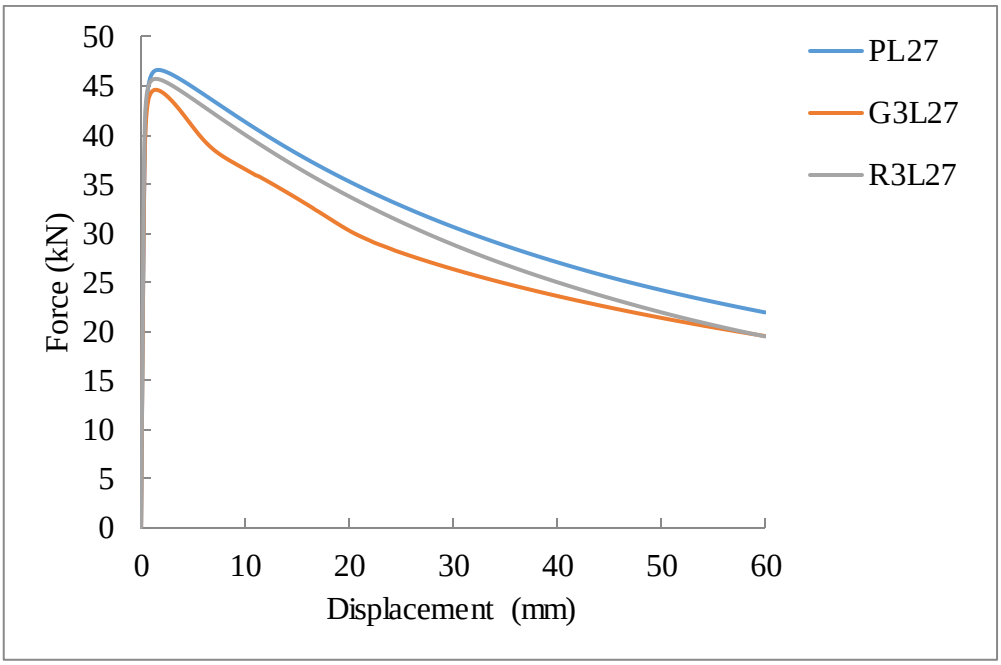

Figure 6.6: Effect of deformation over length for 27 mm length of mechanical anchor

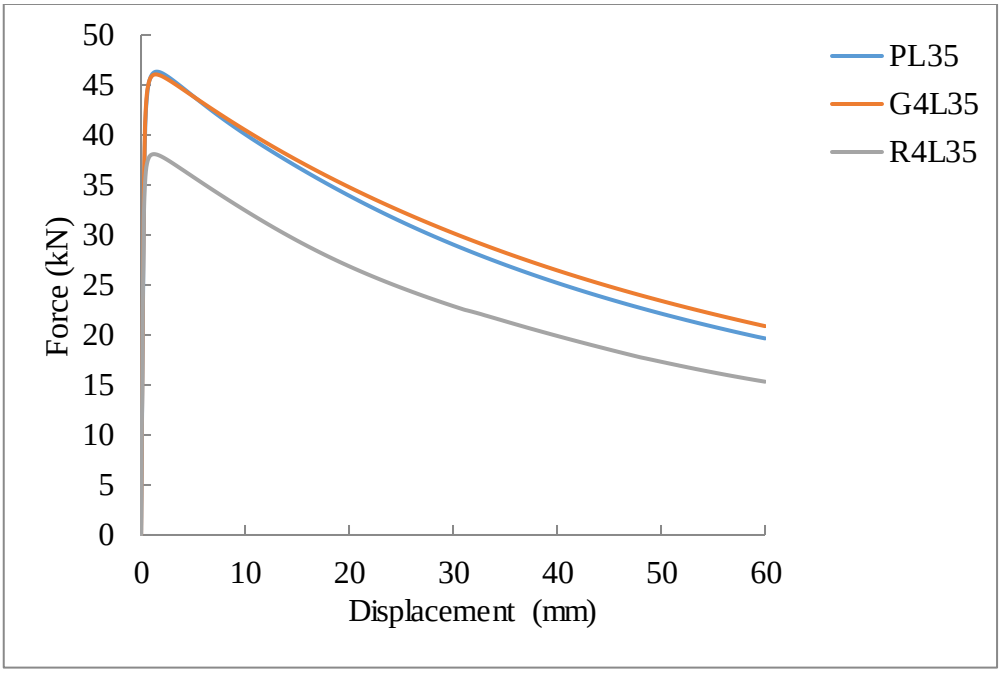

Figure 6.7: Effect of deformation over length for 35 mm length of mechanical anchor

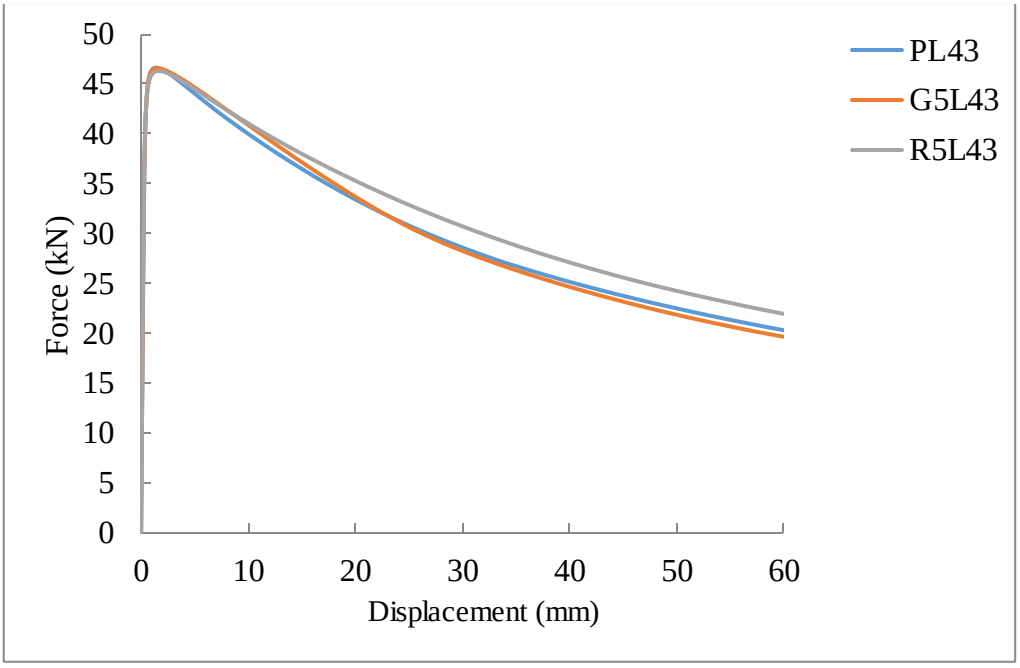

Figure 6.8: Effect of deformation over length for 43 mm length of mechanical anchor

6.2.3 Behaviour of initial cracking to ultimate failure

The crack can be analysed with the help of damage pattern generated within the concrete. As the loading increased, the tensile stress within the concrete and steel were generated. When the tensile stress in the concrete exceeded from the tensile strength of the concrete then the crack

or damage occurs within the concrete. In all the different analysis, it was found that the initial crack appeared near the mechanical anchor. As the load increased, the damage pattern propagated towards the surface. When the stress in the reinforcement exceeded the yield strength of the reinforcement then yielding occurred. The maximum pull-out capacity was found due to yielding of the bar. The failure was bar failure or ductile failure. Approximately at the 5-mm displacement loading, the maximum pull-out force occurred. After the maximum force when the displacement was further increased then yielding occurred but at the lower value of force as compared to the maximum pull-out force. As the displacement loading was again increased then the pull-out force found as lower as 10 to 25 kN for various analysis till 60 mm displacement loading. The initial crack and crack after 60 mm displacement loading (total loading) is shown in Figure 6.9 and 6.10 respectively in the form of damage by red colour notation.

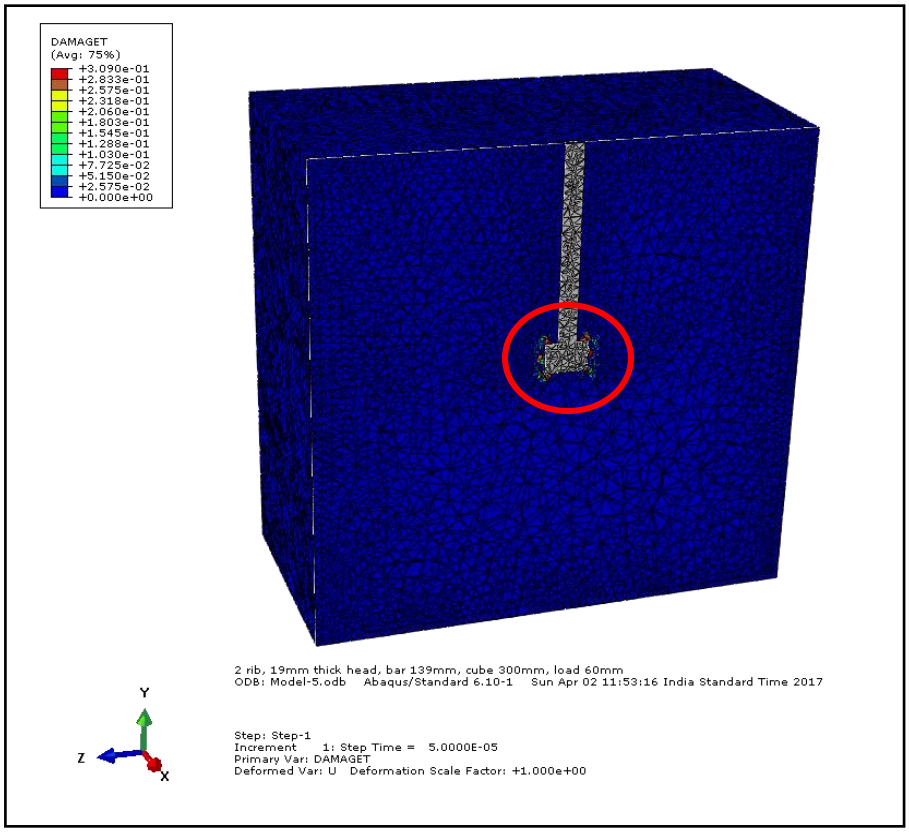

Figure 6.9: Initial crack pattern near mechanical anchor (shown by red circle)

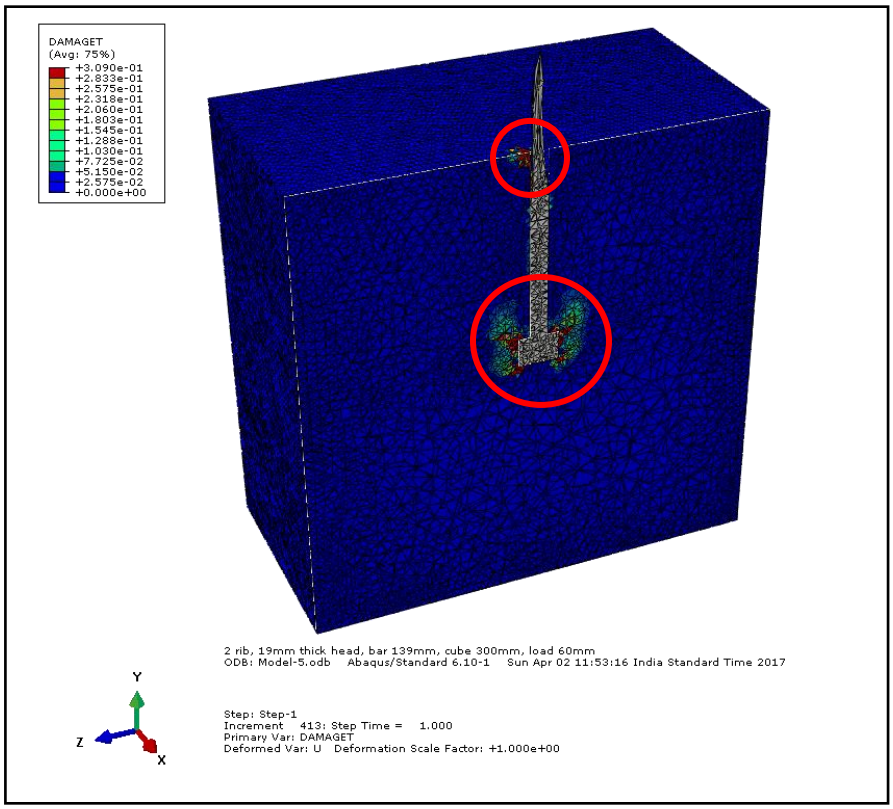

Figure 6.10: Final crack pattern at 60 mm displacement loading (Shown in red circle)

6.3 Experimental results

6.3.1 Pull-out test result with anchor

When the mechanical anchor was used, the bond strength as well as pull-out capacity was very good. During the pull-out testing, the failure mode was bar fracture or ductile failure. It shows that when the anchor was used, the weak zone was in the bar and it break before the concrete failure or pull-cone failure. The failure pattern is shown in Figure 6.11 and 6.12.

Figure 6.11: Failure pattern

a) Fracture portion of bar

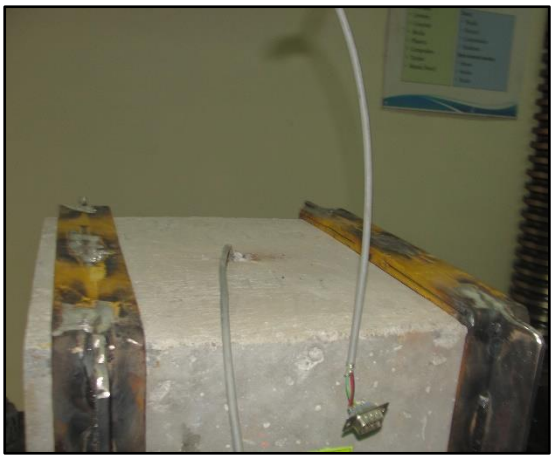

b) Specimen after bar fracture

Figure 6.12: Bar and concrete specimen after failure

The maximum pull-out force for 3 different types of anchor plain, groove and rib with 11 mm length are 65.70 kN, 67.13 kN and 65.10 kN respectively. The displacement at maximum force for PL11, G1L11 and R1L11 are 13.60 mm, 14.72 mm and 17.50 mm respectively. The maximum displacement for PL11, G1L11 and R1L11 are 17.34 mm, 19.49 mm and 21.71 mm respectively. The comparison between force vs displacement curve for PL11, G1L11 and R1L11 are shown in Figure 6.13.

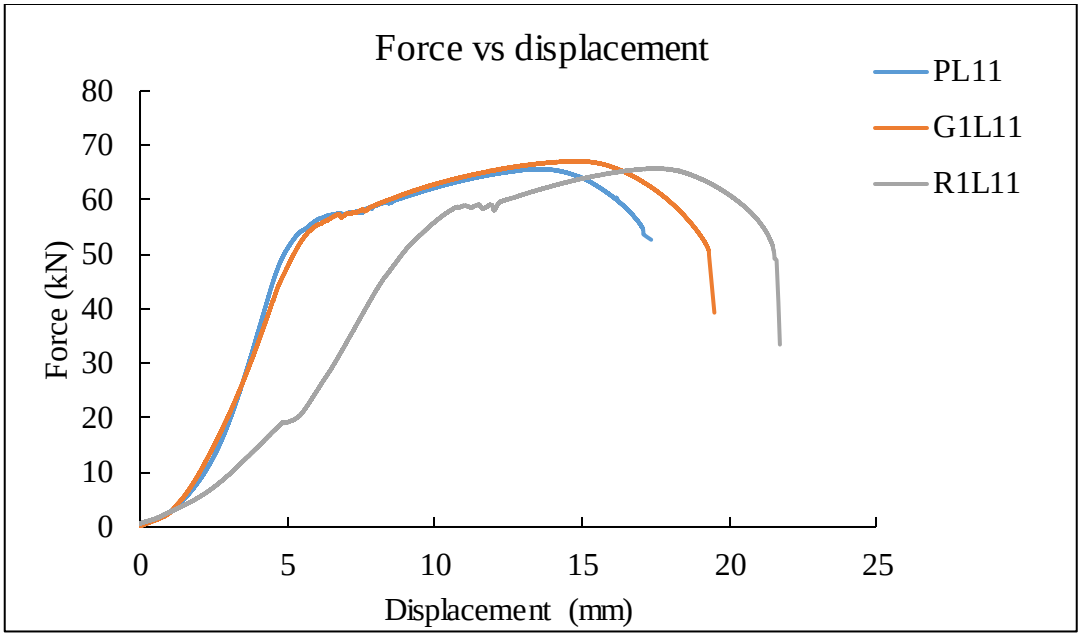

Figure 6.13: Comparison between pull-out capacity of different mechanical anchors

The behaviour of the different mechanical anchors are showing nearly the equivalent pull-out capacity. It is due to the reason that the mode of failure in all the cases were bar fracture. Although the effect of different mechanical anchors can be seen when the failure mode will be pull-cone failure. For the pull-cone failure, there is a need to reduce the embedment depth whatever used in the present study.

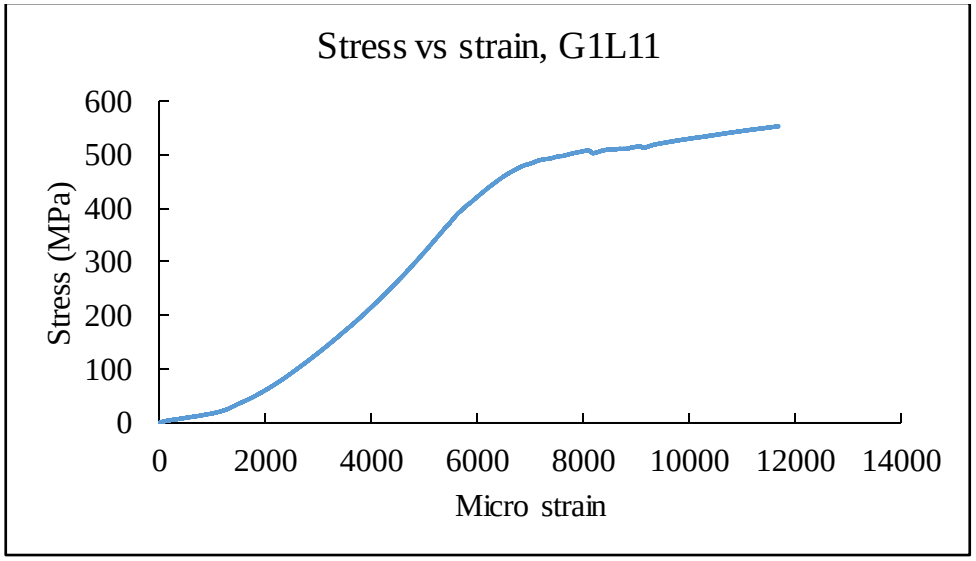

Figure 6.14: Stress-strain behaviour of G1L11 mechanical anchor

The stress-strain behaviour for the strain gauge installed at the reinforcement are of similar type in all the three cases. It is due to the reason that the failure took place in the bar. The

maximum stress generated in PL11, G1L11 and R1L11 were 581.41 MPa, 594.07 MPa and 576.10 MPa respectively. One of the graph for G1L11 is shown in Figure 6.14.

6.3.2 Pull-out result without anchor

A bar with the same embedment was also tested without anchor for the comparison of the result. The mode of failure in this case was observed as first yielding of bar and then slippage of the bar. The failure made a small pull-cone with concrete of approximately diameter of 100 mm near the surface of the concrete. A small cone The failure pattern is shown in Figure 6.15.

Figure 6.15: Failure pattern

a) Bar portion after failure b) Concrete cube after failure

Figure 6.16: Bar and concrete specimen after failure

The maximum pull-out force was observed 62.03 kN. The displacement at maximum force was 10.32 mm. The maximum displacement was 60.39 mm. After that the testing was stopped was by UTM. The maximum stress generated was 548.90 MPa. The force vs displacement curve is shown Figure 6.17.

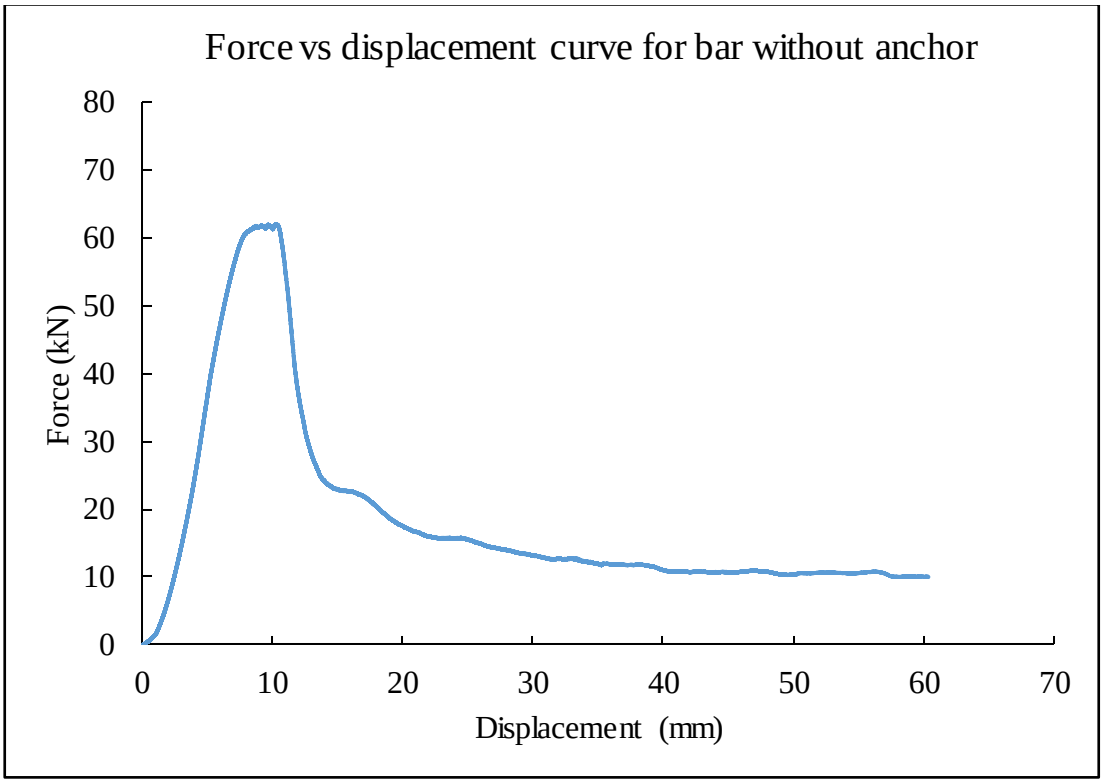

Figure 6.17: Force vs Displacement curve for without anchor

6.3.3 Comparison of results of with and without anchor

While comparing the result between with and without anchor, it can be seen that the failure mode was different in both the cases. In the first case i.e. with anchor, the failure mode is the fracture of bar while in the second case, the failure is due to initially yielding of the bar and then slippage of the bar with small cone of concrete. The load is more in the case of anchor while total displacement is more in the case of without anchor. The displacement at maximum force is less in the case of without anchor.

6.3.4 Effect of length and deformation over length of anchor on pull-out capacity

As the failure mode was bar fracture, the effect of length and deformation over length of mechanical anchor on the pull-out capacity could not estimate at the present study. There is a need to reduce the embedment depth to happen the pull-cone failure.

6.4 Comparison of numerical and experimental results

In section 6.2 and section 6.3, numerical and experimental results are presented. In the numerical analysis, all the 15 types of mechanical anchors are analysed. But in the experimental analysis, the failure mode was bar failure and results were approximately same. Due to this reason, the test was stopped after analysing 1 set of specimen. However, the maximum pull-out capacity in the experimental analysis is 66 kN (average value) whereas in the numerical analysis, the value is 47 kN (average value). In the numerical analysis, the value is less due to the reason that the bar is assumed plain in place of deformed bar and the element type is linear tetrahedron.

CHAPTER 7

CONCLUSIONS AND FUTURE SCOPE OF WORK

7.1 Summary

Due to limited sectional dimensions at beam-column joint and higher stress concentration, a large amount of reinforcement is generally required. This results into congestion of reinforcement, honeycombing in concrete or sometimes inadequate anchorage length due to poor workmanship at beam-column joints, passing vulnerability in RC moment resisting frame. This congestion occurs due to presence of beam as well as column reinforcement in the joint area. This congestion can be reduced by preventing the beam reinforcement from the presence in the beam-column joint area. This can only be possible when the hooked portion of the bar will be cut and some mechanical anchorage system will be used. Such an attempt has been made in the present study. Numerical and experimental analysis are done for selecting the mechanical anchorage system for beam-column joint. For the prime objective, the pull-out capacity of the headed bar, with different type of mechanical anchorage are done. Results are also compared with the bar without anchor.

7.2 Conclusions

Based on the work carried out, following conclusions can be drawn:

- In the experimental investigation, the failure pattern during the pull-out of the bar without anchor is slippage of the bar while the failure pattern of the bar with anchor is the fracture of the bar after yielding with higher pull-out capacity. From these results, it can be concluded that the presence of mechanical anchor significantly modifies the pull-out behaviour of the bar in concrete and increases its pull-out strength.
- From the numerical analysis, it can be concluded that with an increase in the length of the mechanical anchor, there is a little effect on the pull-out capacity of the headed bar.
- The numerical analysis reveals that the presence of ribbed and grooved deformations throughout the length of mechanical anchor has a minimal effect on the pull-out capacity of the headed bar.

7.3 Future scope of work

The following points have been suggested for future research in this area:

- To analyse the effectiveness of different types of mechanical anchor by reducing the embedment depth of the headed bar so that pull-cone failure may occur.
- Experimental investigation of beam-column joint using the effective mechanical anchor found from the pull-out testing and comparison of the same results with the experimental investigation of the beam-column joints with hooked bar.
- Experimental investigation of beam-column joints with mechanical anchor by varying the diameter of the bar, size of the mechanical anchor, grade of concrete and amount of reinforcement and comparison of the same results with the experimental investigation of the beam-column joints with hooked bar.
- Numerical modeling and validation of the experimental results found from the experimental investigation of the beam-column joints.
- Cost comparison with the conventional method of anchorage.
- Performance of the headed bar in light weight concrete and with precast beam-column joint.
- Development of an empirical relation for the dimension of the mechanical anchor.

REFERENCES

ABAQUS (2012). "ABAQUS 6.12 Documentation", *Dassault Systemes Simulia Corporation*, Providence, RI, USA.

ACI 318 (2011). "Building Code Requirements for Structural Concrete" *American Concrete Institute, Detroit, Michigan, US.*

ACI 318 (2014). "Building Code Requirements for Structural Concrete" *American Concrete Institute, Detroit, Michigan, US.*

ACI 408 (2003). "Bond and Development of Straight Reinforcing Bars in Tension" *American Concrete Institute, Detroit, Michigan, US.*

Alaka Oil and Gas Association (2017). Available at: http://www.aoga.org/ [Accessed: 08 August, 2016].

ASTM A970/A970M (2016). "Standard Specification for Headed Steel Bars for Concrete Reinforcement" *ASTM International*, West Conshohocken, pp. 1-9.

Bashandy, T. R. (1996). "Application of Headed Bars in Concrete Members" *PhD Dissertation*, pp.1–318.

Bennett C. D. and Schoffstall W. E. (2006). "Reinforced concrete structure, rebar end anchor therefor and method of manufacturing" U.S. Patent No. 0059841.

Berner D.E. and Hoff D.C. (1994). "Headed Reinforcement in Disturbed Strain Regions of Concrete Members" *Concrete International*, 16(1), pp.48–52.

Caldentey, A. P., Marchetto F., Peiretti, H. C. and Villareal J. I. (2013). "Plate-anchored reinforcement bars: A new simple and physical model for practical applications" *Engineering Structures*, 52, pp.168–178.

Chun, S.C., Oh B., Lee S. H. and Naito C. J. (2009). "Anchorage strength and behaviour of headed bars in exterior beam-column joints" *ACI Structural Journal*, 106(5), pp.579–590.

Darwin, D. and Graham, E.K., (1993). Effect of Deformation Height and Spacing on Bond Strength of Reinforcing Bars. Report.

DeVries, R.A., 1996. "Anchorage of Headed Reinforcement in Concrete" *PhD Dissertation*, pp.1–314.

Dhake P. D., Patil Y. D. and Patil H. S. (2015). "Anchorage behaviour and development length of headed bars in exterior beam – column joints" *Magazine of Concrete Research*, 67(2), pp.53–62.

Dilger, W.H. and Ghali, A. (1981). "Shear Reinforcement for Concrete Slabs," *ASCE Journal of Structural Engineering*, 107(12), pp. 2403-2420.

Fuchs W., Eligehausen R. and Breen J. E. (1995). "Concrete Capacity Design Approach for Fastening to Concrete" *ACI Structural Journal*, 92 (1), pp. 73-94.

Goto Y., K. Nishimura, H. and Yamazaki, A.K. (2012) "Anchorage Failure and Shear Failure of RC Exterior Beam-Column Joint" *15th World Conference on Earthquake Engineering (15WCEE)*.

Gruson P. and Kies A. M. (2001). "Bar anchor and method for reinforcing steel in concrete construction" U.S. Patent No. 6286270.

Guido Dhondt (2014). "Four-node tetrahedral element (C3D4 and F3D4)" Available at: http://web.mit.edu/calculix_v2.7/CalculiX/ccx_2.7/doc/ccx/node32.html [Accessed: 10 July, 2016].

Hiendl H. (1992). "Reinforcing steel connection" U.S. Patent No. 5131204.

Hong, S.G., Chun S. C., Lee S. H. and Oh B. (2007). "Strut-and-Tie model for development of headed bars in exterior beam-column joint" *ACI Structural Journal*, 104(5), pp.590–600.

IS 13920 (2016). "Ductile detailing of reinforced concrete structures subjected to seismic forces". *Bureau of Indian Standards, New Delhi, India.*

IS 2386-I (1963). "Methods of test for aggregates for concrete" *Bureau of Indian Standards, New Delhi, India.*

IS 2770-I (1967). "Method of testing bond in reinforced concrete" *Bureau of Indian Standards, New Delhi, India.*

IS 4031-II (1999). "Methods of physical tests for hydraulic cement" *Bureau of Indian Standards, New Delhi, India.*

IS 4032 (1985). "Method of chemical analysis of hydraulic cement" *Bureau of Indian Standards, New Delhi, India.*

IS 456 (2000). "Plain and Reinforced Concrete Code of Practice" *Bureau of Indian Standards, New Delhi, India.*

IS 8112 (2013). "Specification for 43 grade ordinary Portland cement" *Bureau of Indian Standards, New Delhi, India.*

Jeffrey L. Wright, S.L.M. (1997). "The Development Length and Anchorage Behaviour of Headed Reinforcing Bars" Report, pp.1–153.

Joint ACI-ASCE Committee 352 (2002), "Recommendations for Design of Beam-Column Connections in Monolithic Reinforced Concrete Structures" *American Concrete Institute, Detroit, Michigan, US.*

Kang, T. H. K. and Mitra, N. (2012). "Prediction of performance of exterior beam-column connections with headed bars subject to load reversal" *Engineering Structures,* 41, pp.209–217.

Kang, T. H. K., Ha, S. S. and Choi, D. U. (2010). "Bar pull-out tests and seismic tests of small-headed bars in beam-column joints" *ACI Structural Journal,* 107(1), pp.32–42.

Kang, T. H. K., Shin M. Mitra N. and Bonacci J. F. (2009). "Seismic Design of Reinforced Concrete Beam-Column Joints with Headed Bars" *ACI Structural Journal,* (106).

Kies A. M., Harry C., Nieuwelaar V. D. and Bowmer G. M. (1989). "Method for rolling tapered threads on bars" U.S. Patent No. 4870848.

Lancelot III, H. B. and Brown, S. B. (2002). "End anchors" U.S. Patent No. 0189175 A1.

Mander J. B., Priestley M. J. N. and Park R. (1988). "Theoretical stress-strain model for confined concrete" *Journal of structural engineering, ASCE*, 114(8), pp. 1804-1826.

Marchetto, F., Caldentey, A. P. and Peiretti, H. C. (2016). "Structural performance of corner joints subjected to a closing moment using mechanical anchorages: an experimental study" Structural Concrete, 17(6), pp.987-1002.

McMackin, P.J., Slutter, R.G., and Fisher, J.W. (1973). "Headed Steel Anchor Under Combined Loading," *AISC Engineering Journal,* 10(2) pp. 43-52.

Mokhtar, A.S., Ghali, A., and Dilger, W.H. (1985). "Stud Shear Reinforcement for Flat Concrete Plates," *Journal of the American Concrete Institute, Proceedings*, 82(5), pp. 676-683.

Murty, C.V.R. (2005). "Earthquake tips", *Indian Institute of Technology Kanpur, India*.

Nayal R. and Rasheed H. A. (2006). "Tension stiffening model for concrete beams reinforced with steel and FRP bars" Journal of materials in civil engineering, *ASCE*, 18(6), pp. 831-841.

Office of the Registrar General & Census Commissioner, India. (2011) "Census data". Available at: http://www.censusindia.gov.in/ [Accessed: 08 March 2017].

Park H. K., Yoon Y. S. and Kim Y. H. (2003). "The effect of head plate details on the pull-out behaviour of headed bars" *Magazine of Concrete Research*, 55(6), pp.485–496.

Pentair (2017). "Lenton Terminator for rebar anchorage" Available at: https://www.erico.com/catalog/literature/CP7E-WWEN.pdf [Accessed: 06 July 2016].

PMINDIA. (2017) "Housing for All by 2022 Mission – National Mission for Urban Housing". Available at: http://www.pmindia.gov.in/en/news_updates/housing-for-all-by-2022-mission-national-mission-for-urban-housing/ [Accessed: 08 March 2017].

Rajagopal S., Prabavathy and Kang T. H. K. (2014). "Seismic behavior evaluation of exterior beam-column joints with headed or hooked bars using nonlinear finite element analysis" *Earthquakes and Structures*, 7(5), pp. 861-875.

Samas M. V. and Ricker E. D. (1992). "Taper thread cutting machine and method" U.S. Patent No. 5158404.

Sengupta, P. and Li, B. (2013). "Modified Bouc–Wen model for hysteresis behaviour of RC beam–column joints with limited transverse reinforcement" *Engineering Structures*, 46, pp.392-406.

Stoker, J.R., Boulware, R.L., Crozier, W.F., and Swirsky, R.A. (1974). "Anchorage Devices for Large Diameter Reinforcing Bars," Caltrans Report (No. CA-DOT-TL-6626-1-73-30).

Thompson MK, Jirsa James O, Breen JE and Klingner RE. (2002) "Anchorage behaviour of headed reinforcement. Literature review"(No. FHWA/TX-0-1855-1).

Uma, S.R. and Prasad, A.M. (1996). "Seismic behaviour of beam column joints in reinforced concrete moment resisting frames", *Department of Civil Engineering, Indian Institute of technology Madras, Chennai*.

Wallace, J. W., Mc Connell S. W., Gupta P. and Cote P.A. (1998). "Use of Headed Reinforcement in Beam-Column Joints Subjected to Earthquake Loads" *ACI Structural Journal*, 95. pp. 590-602.

Wu, J. Y., Li, J and Faria, R. (2006). "An energy release rate-based plastic –damage model for concrete" *International Journal of solids and structure*, 43(3), 583-612.